Proc. NIPR Symp. Antarct. Meteorites, **6**, 204–233, 1993

PETROLOGY AND MINERALOGY OF CK CHONDRITES: IMPLICATIONS FOR THE METAMORPHISM OF THE CK CHONDRITE PARENT BODY

Takaaki NOGUCHI

Department of Earth Sciences, Faculty of Science, Ibaraki University, 1–1, Bunkyo 2-chome, Mito 310

Abstract: The petrology and mineralogy of four CK chondrites, Karoonda (CK4), Maralinga (CK4), Yamato(Y)-693 (CK4), and Elephant Moraine (EET)87507 (CK5) were investigated in detail to estimate the origin of their quite heterogeneous plagioclases and the metamorphic history of CK chondrite parent body. EPMA analyses and SEM observations revealed that plagioclases in chondrules, CAIs, and matrices in CK chondrites have different compositional variations and that plagioclases in matrices display distinct reverse zoning in regard to An content. Cores of matrix plagioclases ($An_{20} \sim An_{40}$) may have formed by recrystallization of primary plagioclases. Rims of matrix plagioclases were probably formed during metamorphism, because the reverse zoning can be observed, regardless of degree of recrystallization. The occurrences and compositions of pyroxenes are different among less recrystallized CK chondrites and recrystallized CK chondrites. Low-Ca pyroxenes in recrystallized matrices are enclosed in matrix plagioclases and different in CaO and Al_2O_3 contents from those in chondrules. Compositions of low-Ca pyroxenes in matrix plagioclases suggest that they include Fe^{3+}. They were probably formed during metamorphism under high oxygen fugacities. Highly oxidized metamorphic conditions are supported by the existence of Fe^{3+} in spinels and high NiO contents in olivines. Olivine-spinel geothermometry and pyroxene compositions suggest that Maralinga, Y-693, EET87507, and some fragments in Karoonda were heated to the temperatures as high as those of type 5 to 6 ordinary chondrites (750 to 850°C). Slow cooling below ~400°C of these meteorites was estimated by sulfide mineral assemblages. Because Maralinga has many different properties from other CK chondrites investigated, it is an anomalous CK chondrite.

1. Introduction

Recently KALLEMEYN *et al.* (1991) proposed a new chemical group of carbonaceous chondrites, CK chondrites, named after the Karoonda meteorite. Bulk compositional data of CK chondrites show that their refractory lithophile and refractory siderophile abundances are intermediate between CV and CO chondrites, and that their volatile abundance pattern is similar to the CV pattern. All the CK chondrites are metamorphosed chondrites. Therefore, they are important for the study of the metamorphism of a carbonaceous chondrite parent body.

CK chondrites have different mineralogy and petrology from those in other chondrites. Mineralogy and petrology of CK chondrites have been investigated by some

researchers (*e.g.*, GEIGER and BISCHOFF, 1989a, b, 1990, 1991a, b; GEIGER *et al.*, 1992; KELLER, 1992; KELLER *et al.*, 1992). GEIGER and BISCHOFF (1991) summarized some unique properties of CK chondrites. (1) The most abundant opaque mineral is magnetite, which includes ilmenite and spinel exsolution lamellae. (2) The chemical composition of plagioclase is quite heterogeneous, $\sim An_{20}$ to $\sim An_{75}$. In some cases, the composition exceeds this range. (3) The NiO content of olivine is high, 0.3–0.7 wt%. (4) Platinum-group-minerals (PGMs) exist in opaque mineral inclusions or grains which are composed of magnetite, pentlandite, monosulfides, and pyrite. Among these features, (1) and (3) are related to the oxidized conditions which the CK chondrites experienced. On the contrary, the origin of heterogeneous plagioclase is not evident. RUBIN (1992) stated that the ubiquitous blackening caused by abundant magnetites and the heterogeneity of plagioclase composition resulted from shock-metamorphism by analogy with shocked ordinary chondrites. In a study of shock intensity, however, SCOTT *et al.* (1991) stated that these features seem not to have resulted from shock-metamorphism.

In this study, I present petrologic and mineralogical data of four CK chondrites, Karoonda (CK4), Maralinga (CK4), Yamato(Y)-693 (CK4), and Elephant Moraine (EET)87507 (CK5). The cause of the heterogeneous plagioclase and the thermal history of CK chondrites will be explored.

2. Materials and Methods

Polished thin sections (PTS') of the following CK chondrites were studied using a scanning electron microscope (SEM) and electron probe microanalyzer (EPMA): Karoonda , CK4 (3970-1); Maralinga, CK4; Y-693, CK4 (92-1); EET87507, CK5 (22). A detailed SEM observation was carried out with a JEOL JSM-840 equipped with an energy dispersive spectrometer (Link system). EPMA analyses were performed by JEOL JXA-733 microprobes operated at 15 kV accelerating voltage and 4 to 9 nA beam current. Correction by the Bence and Albee method was used for the analyses of silicates, oxides, and phosphates, and the ZAF method for sulfides. A special deconvolution program was applied to correct for X-ray overlaps of K_β and K_α lines between some elements such as Ti and V, Ca and P, Cu and Ni, Cu and Co, Cu and Fe, S and Co, and Co and Fe.

3. Results

3.1. Petrography

3.1.1. Overall texture

Thin sections of Karoonda, Maralinga, Y-693, and EET87507 show that there are some textural differences among them. The most obvious difference is the degree of integration of chondrules into marices. In Karoonda and Maralinga, chondrules are well defined. On the other hand, in Y-693 and EET87507, many chondrules are integrated into matrices but some chondrules are readily discernible. Outlines of chondrules are less definite in EET87507 than in Y-693.

The three chondrites other than Karoonda are compact meteorites. However, the overall texture of Karoonda suggests that this meteorite is composed of fragmental materials as reported by SCOTT and TAYLOR (1985) and BREARLEY *et al.* (1987). They

reported that some grains of olivine and plagioclase appeared to be fragments of larger grains and suggested brecciation after metamorphism. Although many fragmental materials in the matrix of Karoonda seem to have been derived from chondrules, there are also many fragmental materials which seem not to have derived from chondrules.

There are no fine-grained opaque matrices in these chondrites. Therefore, the term "matrix" in this paper is used for materials which occupy the space between the well defined components such as chondrules and inclusions. Silicate minerals in matrices, and in chondrules in a lesser degree, are blackened by many fine-grained magnetites, most of which are $<$a few μm.

3.1.2. Chondrules

(a) General description

Grain sizes of chondrules in CK chondrites are as large as those in CV chondrites. Most of chondrules in these meteorites are 0.5 to 1 mm in diameter. Porphyritic olivine (PO), porphyritic olivine pyroxene (POP), and barred olivine (BO) chondrules were observed in Karoonda. In Maralinga, PO chondrules were dominant, and POP and BO chondrules were rare. In Y-693 and EET87507, some PO chondrules were recognized.

The proportion of mesostasis to crystals in a chondrule in these CK chondrites is smaller than that in other carbonaceous chondrites. Figure 1a displays a backscattered electron image (BEI) of a PO chondrule in Maralinga. Traces of voids and tiny opaque grains ($<$a few μm across) delineate original outlines of the olivine crystals. They suggest overgrowth of olivine on olivine microphenocrysts.

Mesostases in chondrules are composed mainly of plagioclase with a minor amount of magnetite (<1 μm in diameter). In some chondrules, mesostases also contain augite and olivine in addition to plagioclase and magnetite.

(b) Patchy or lamellae-like pyroxene zoning in POP chondrules in Karoonda

POP chondrules were often observed in Karoonda. Low-Ca pyroxenes in POP chondrules show the patchy or lamellae-like Fe-Mg zoning. Figure 1b shows a BEI photograph of a POP chondrule which contains magnesian low-Ca pyroxenes. In this figure, En contents in dark patches are $>En_{90}$, and those in brighter patches are $\sim En_{75}$. This type of zoning was observed in some type-3 (TSUCHIYAMA *et al.*, 1988) and -4 ordinary chondrites (L4: NOGUCHI, 1987; LL4: MCCOY *et al.*, 1991), and in some Carlisle-Lakes-type chondrites (WEISBERG *et al.*, 1991).

Low-Ca pyroxenes which contain small dark patches and have high Fs contents ($<En_{75}$) in bright patches tend to be porous or fibrous (Fig. 1c). Such porous low-Ca pyroxenes do not occur in ordinary and Carlisle-Lakes-type chondrites. The formation of such porous or fibrous pyroxenes could not have formed only by the increase of Fs content, because the increase of Fs content results in $\sim$2% volume increase.

(c) Replacement of low-Ca pyroxene by olivine in POP chondrules in Maralinga

Although augite was often observed in PO chondrules, chondrules which contain porphyritic low-Ca pyroxenes are rare in Maralinga. Low-Ca pyroxenes in POP chondrules are surrounded by olivine, and such olivine is also observed along the *c*-axis of low-Ca pyroxenes (Fig. 1d). Thin layers of augite ($<$several μm thick) are observed along the boundaries between the low-Ca pyroxenes and the olivines. Such augites do not contain tiny magnetite inclusions which are common in rim augites on the low-Ca pyroxenes. Rim augites are not surrounded by olivine.

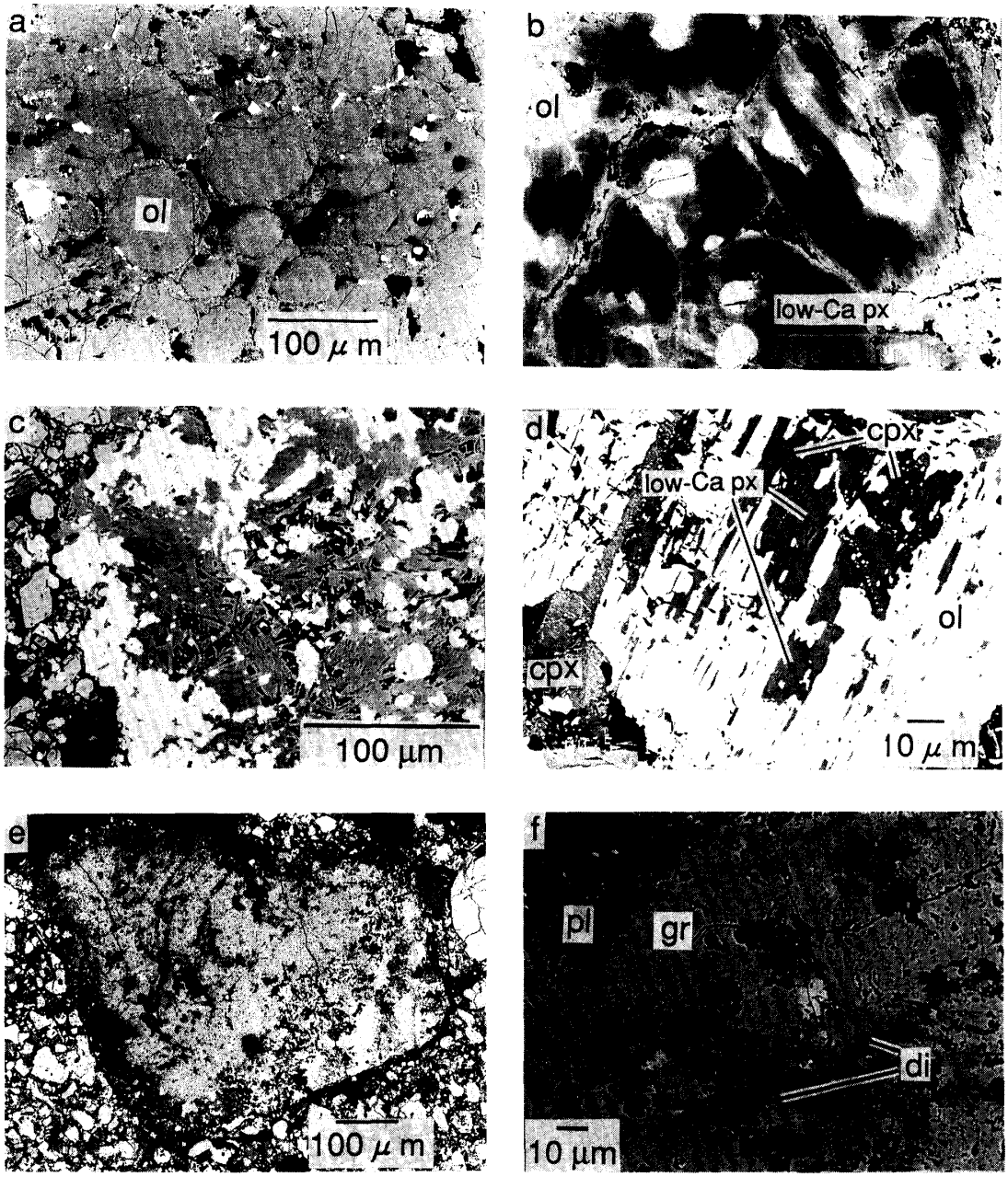

Fig. 1. Backscattered electron images (BEIs) of various textures shown in CK chondrites. a. A PO chondrule in Maralinga. Overgrowth of olivine on olivine microphenocrysts can be inferred from the traces of voids and tiny opaque minerals. ol: olivine. b. Patchy or lamellae-like Fe-Mg zoning in low-Ca pyroxene in a POP chondrule in Karoonda. ol: olivine; low-Ca px: low-Ca pyroxene. c. Aggregate of acicular low-Ca pyroxenes in a chondrule in Karoonda. Pyroxenes in this chondrule are more ferrous than that in Fig. 1b. d. Replacement texture of low-Ca pyroxene by olivine in Maralinga. Thin augite layers exist along the boundaries between low-Ca pyroxene and olivine. In lower left of this photograph, rim augite on low-Ca pyroxene is shown. It includes many fine-grained opaque particles (probably magnetite). ol: olivine; low-Ca px: low-Ca pyroxene; cpx: augite. e. A grossular-bearing CAI in Karoonda. f. An enlarged view of the grossular-bearing CAI (Fig. 1e). Grossular forms fine-grained compact aggregate, and overgrowth of diopside is shown. gr: grossular; di: diopside; pl: plagioclase.

This texture is interpreted as the replacement of low-Ca pyroxene by olivine. The replacement progressed on the peripheries and along the *c*-axis of the pyroxene crystals and augite was concentrated along the reaction fronts. The replacement texture was not obvious in low-Ca pyroxene crystals which are set within chondrules and completely surrounded by olivine. However, augite was observed along the boundaries between olivines and low-Ca pyroxenes within chondrules. Therefore, the replacement reaction probably occurred between all the low-Ca pyroxenes and olivines.

A texture which indicates replacement of low-Ca pyroxene by olivine was reported in Allende (*e.g.*, HOUSLEY and CIRLIN, 1983; NOGUCHI, 1989). In Allende, the replacement texture is closely related to Fe-Ni metal grains in chondrules. The replacement texture in Allende clearly shows that the texture was formed by the reaction between low-Ca pyroxene and Fe-Ni metal. In Maralinga, it is implausible that the reaction between low-Ca pyroxene and Fe-Ni metal occurred and that the metal was subsequently oxidized to magnetite during metamorphism, because magnetite does not closely occur with the two minerals displaying the replacement texture. Another difference between the replacement textures is that there is no augite along the boundaries between low-Ca pyroxene and olivine in Allende. These differences may have been related to the different FeO-supplying phases (magnetite or Fe-Ni metal).

3.1.3. CAIs

(a) General description

KALLEMEYN *et al.* (1991) stated that CAIs are rare in CK chondrites. In Karoonda, two CAIs were observed in a PTS with about $\sim 220\,mm^2$. In EET87507, one CAI was observed in a PTS with about $\sim 140\,mm^2$. However, in Y-693, no CAI was found because of a small PTS with $\sim 15\,mm^2$. On the contrary, Maralinga contains more CAIs than other CK chondrites investigated. Six CAIs were observed in a PTS with $\sim 220\,mm^2$. KELLER *et al.* (1992) reported that Maralinga contained more CAIs than other CK chondrites. This observation is consistent with theirs.

These CAIs commonly contain plagioclase, aluminous spinel, augite, and magnetite. But in addition to these minerals, other minerals such as olivine (in Maralinga and EET87507), Ca-phosphate (in Maralinga), and grossular (in Karoonda) were also observed.

(b) CAIs in Karoonda: Discovery of a grossular-bearing CAI

Two CAIs were observed. One is small ($\sim 150\,\mu m$ across) and irregular, and is composed of spinel, plagioclase, magnetite and augite. This inclusion consists of three layers. The innermost core is composed of aluminous spinel, magnetite, and interstitial plagioclase. The intermediate layer is composed of plagioclase including tiny ($< 1\,\mu m$) spinel inclusions. The outermost layer is composed of a rim of augite ($\sim 10\,\mu m$ thick). It is similar to the spinel-pyroxene inclusions in CM chondrites, which are the most numerous among refractory inclusions in CM chondrites (MACPHERSON *et al.*, 1988) and the type-3 inclusions in Maralinga which were described by KELLER (1992).

Another is large ($\sim 700\,\mu m$ across) and subrounded (Fig. 1e). This inclusion seems to have been a fragment of a larger one, because a part of this inclusion lacks a rim which is composed mainly of plagioclase. This inclusion comprises grossular, aluminous spinel and interstitial plagioclase with small amounts of magnetite and augite (diopsite). There are two areas in which the main minerals are anhedral spinel and grossular,

respectively. Anhedral spinels contain many tiny (<a few μm across) magnetites, and some spinels are $\sim$100 μm across. Grossular forms compact aggregates and does not contain many inclusions. Grossular is surrounded by rims of augite (<10 μm thick) and the interstices of them are filled with plagioclase containing a minor amount of tiny magnetite (<a few μm across) (Fig. 1f).

(c) CAIs in Maralinga

KELLER (1992) described the petrology and mineralogy of CAIs in this meteorite in detail. Therefore, I describe CAIs only briefly in this paper. They contain various amounts of plagioclase, aluminous spinel, augite, magnetite, olivine, magnetite, and Ca-phosphate. They show various textures, and KELLER (1992) described four types of CAIs. All of them were observed in a PTS used in this study. There are some inclusions composed of plagioclase with a minor amount of magnetite. Although those plagioclase inclusions could not be classified as CAIs, the compositional range of plagioclase in them overlaps that in CAIs.

(d) CAIs in EET-87507

A large ($\sim$600 μm across) subrounded CAI was observed. It consists of euhedral aluminous spinel, augite, magnetite, and interstitial plagioclase. Although the grain size of spinel varies from several to $\sim$50 μm, their composition is homogeneous. On the other hand, augite shows compositional zoning. Their Al_2O_3 content decreases from core (>15 wt%) to rim ($\sim$10 wt%). Plagioclase contains a fairly high amount of an albite component, and shows narrow compositional variation (An_{75} to An_{80}).

3.1.4. Matrix

(a) General description

The matrices of Karoonda, Maralinga, and Y-693 are composed of olivine, plagioclase, opaque minerals (mainly magnetite and rare sulfides), and pyroxenes. The abundance of pyroxenes in Maralinga is very low. The grain sizes of plagioclases in the matrices are variable among these chondrites. The range of grain sizes of matrix plagioclases is from $\sim$10 to $\sim$100 μm across in Karoonda, some grains exceed 100 μm across. In Maralinga, most of the matrix plagioclases are 20 to 50 μm across. Compared with them, Y-693 and EET87507 are much more recrystallized than Karoonda and Maralinga. Therefore, matrix minerals in them are coarser than those in the two previous chondrites, and boundaries between chondrules and matrix are poorly defined. Many matrix plagioclases exceed 100 μm across in them, and some matrix plagioclases in EET87507 exceed 200 μm across.

The cores of matrix plagioclases contain more inclusions than the rims of matrix plagioclases. Inclusions are acicular pyroxenes (both low-Ca and augite), small magnetite grains (<10 μm across), and olivine. Acicular pyroxenes are the characteristic matrix minerals in CK chondrites except for Maralinga, and their occurrence is closely related to matrix plagioclase. In most cases, they are included in matrix plagioclases (Fig. 1g). However, matrix plagioclases in Maralinga rarely contain low-Ca pyroxene.

Calcite and calcite-magnetite inclusions (<10 μm across) were observed in the matrix of Maralinga. These inclusions were perhaps formed by weathering on the earth as KELLER (1992) insisted. But it is not necessarily clear that such inclusions could be formed by terrestrial weathering.

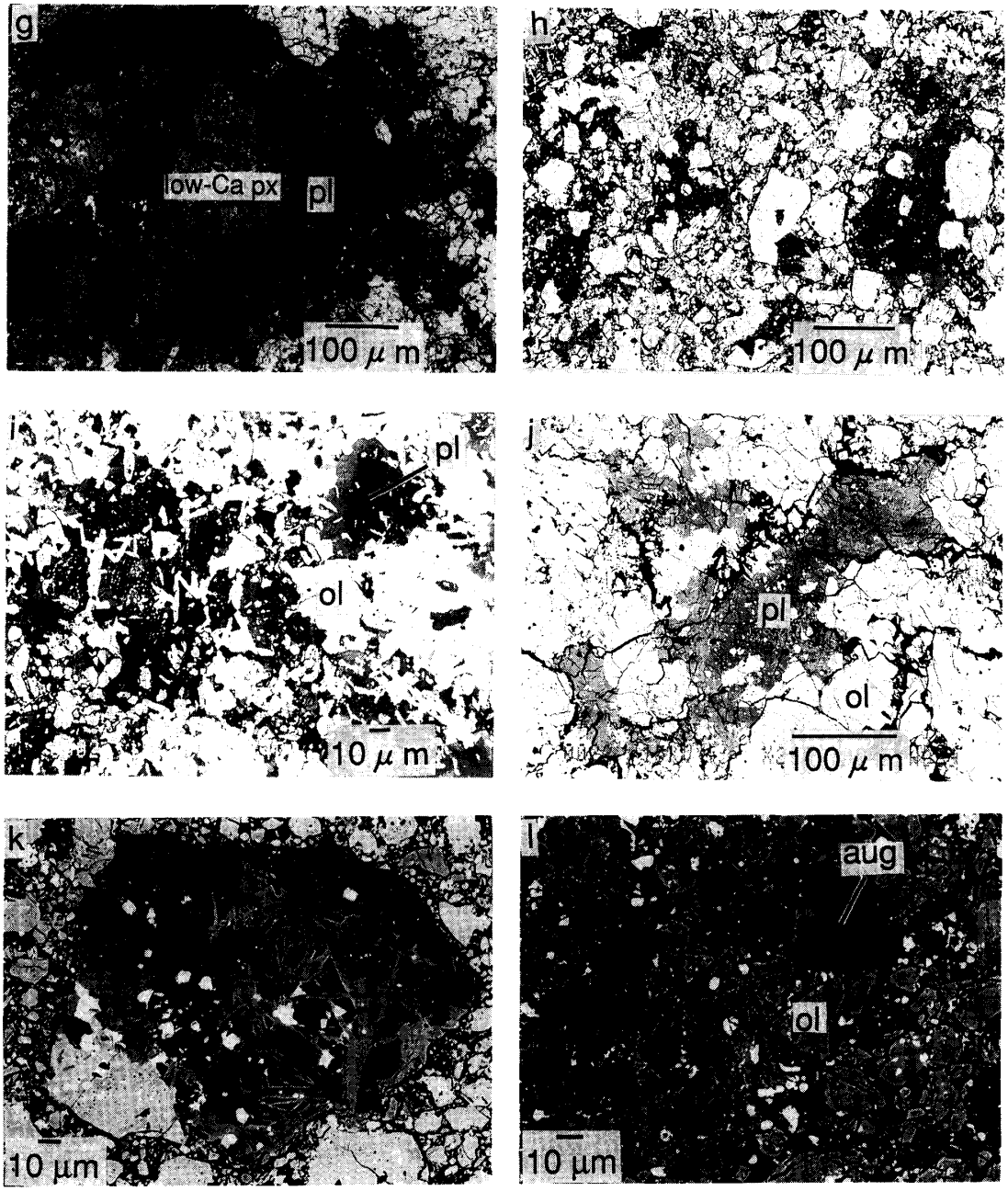

Fig. 1 (Continued).

g. Low-Ca pyroxenes are enclosed in matrix plagioclase in EET87507. This is a typical occurrence of low-Ca pyroxenes in recrystallized CK chondrites. low-Ca px: low-Ca pyroxene; pl: plagioclase. h. Matrix plagioclases in Karoonda. A plagioclase grain in the right of the photograph show reverse zoning with sharp boundaries. i. Matrix plagioclases in Maralinga. A plagioclase grain in the upper right of the photograph shows reverse zoning with sharp boundaries. ol: olivine; pl: plagioclase. j. Matrix plagioclase in Y-693. Grain sizes of plagioclases are larger than that in Figs. 1i and j. Peripheries of the plagioclase grains are more calcic than the cores. But boundaries between cores and rims are gradual. ol: olivine; pl: plagioclase. k. A clast in Karoonda. It shows that acicular pyroxenes are enclosed in plagioclase. l. Fs-rich augite in matrix in Karoonda. It shows Fe-Mg zoning. ol: olivine; aug: augite.

(b) Reverse zoning of matrix plagioclase

In Karoonda, matrix plagioclases which are >several tens of μm across have calcic rims of about 10 μm thick with sharp boundaries (Fig. 1h). In this figure, the An content varies outward from $\sim An_{40}$ to $\sim An_{75}$ within intervals of $<10\,\mu$m. But most of the smaller plagioclase grains do not show remarkable compositional zoning, and both calcic and sodic plagioclases are observed. Matrix plagioclases in Maralinga have calcic rims of 5–10 μm thick with sharp boundaries as well as those in Karoonda (Fig. 1i). The An content varies outward from $\sim An_{40}$ to $\sim An_{80}$ within intervals of $<10\,\mu$m. Although matrix plagioclases in Y-693 and EET87507 are much larger than those in Karoonda and Maralinga, they also show reverse zoning (Fig. 1j). However, the zoning is relatively gradual and matrix plagioclases which show a sharp change of composition are rare.

(c) Two types of fragments suggesting different origins in matrix in Karoonda

The fragmentary appearance of matrix minerals and larger objects such as chondrules was observed in Karoonda. Textures of large fragments with $>100\,\mu$m across suggest that there are at least two types of fragments in matrix: fragments derived from chondrules, and fragments which are characterized by plagioclase including acicular pyroxenes and tiny magnetites (Fig. 1k). The latter fragments are similar to matrix plagioclases including pyroxenes in recrystallized CK chondrites such as Y-693 and EET87507. Actually low-Ca pyroxenes in this type of fragment have similar compositions to those in low-Ca pyroxenes in matrix plagioclases in Y-693 and EET87507. Therefore, Karoonda seems to contain fragments derived from more recrystallized CK materials along with less recrystallized CK materials.

(d) Ferrosilite-rich augite in matrix and chondrules in Karoonda

In the matrix of Karoonda, relatively small (< a few tens μm across) augite crystals are observed (Fig. 1l). They are directly set among matrix minerals and not enclosed in matrix plagioclases. They often show compositional zoning of FeO content. These augites have different compositions from rim augites on low-Ca pyroxenes in chondrules (Fig. 2a). Even in chondrules, augites with a similar texture and similar composition are observed. They are anhedral and sometimes coexist with anhedral olivines. These crystals fill interstices of microphenocrysts of olivine and pyroxene. In Maralinga, augites were also observed in the matrix. However, the augites have a similar composition to the augite rims on low-Ca pyroxenes in chondrules.

(e) Coarse grained matrices in Y-693 and EET87507

Y-693 and EET87507 are more recrystallized meteorites; their grain sizes of matrix plagioclases are larger than those in the previous two meteorites. In Y-693 and EET87507, the occurrences of low-Ca pyroxenes are almost restricted to matrices. Both thin acicular ($<10\,\mu$m wide) and anhedral pyroxenes are observed in matrix plagioclases (Fig. 1g). Both low-Ca pyroxene and augite appear in both occurrences.

In EET87507, many large anhedral pyroxenes ($<400\,\mu$m across) are included in matrix plagioclases. The pyroxenes often include plagioclases almost parallel to the *c*-axis of pyroxene (Fig. 1m). The texture of this pyroxene probably suggests the replacement of pyroxene by plagioclase.

3.1.4. Isolated opaque inclusions

There are two generations of magnetites in the CK chondrites (*e.g.*, GEIGER and

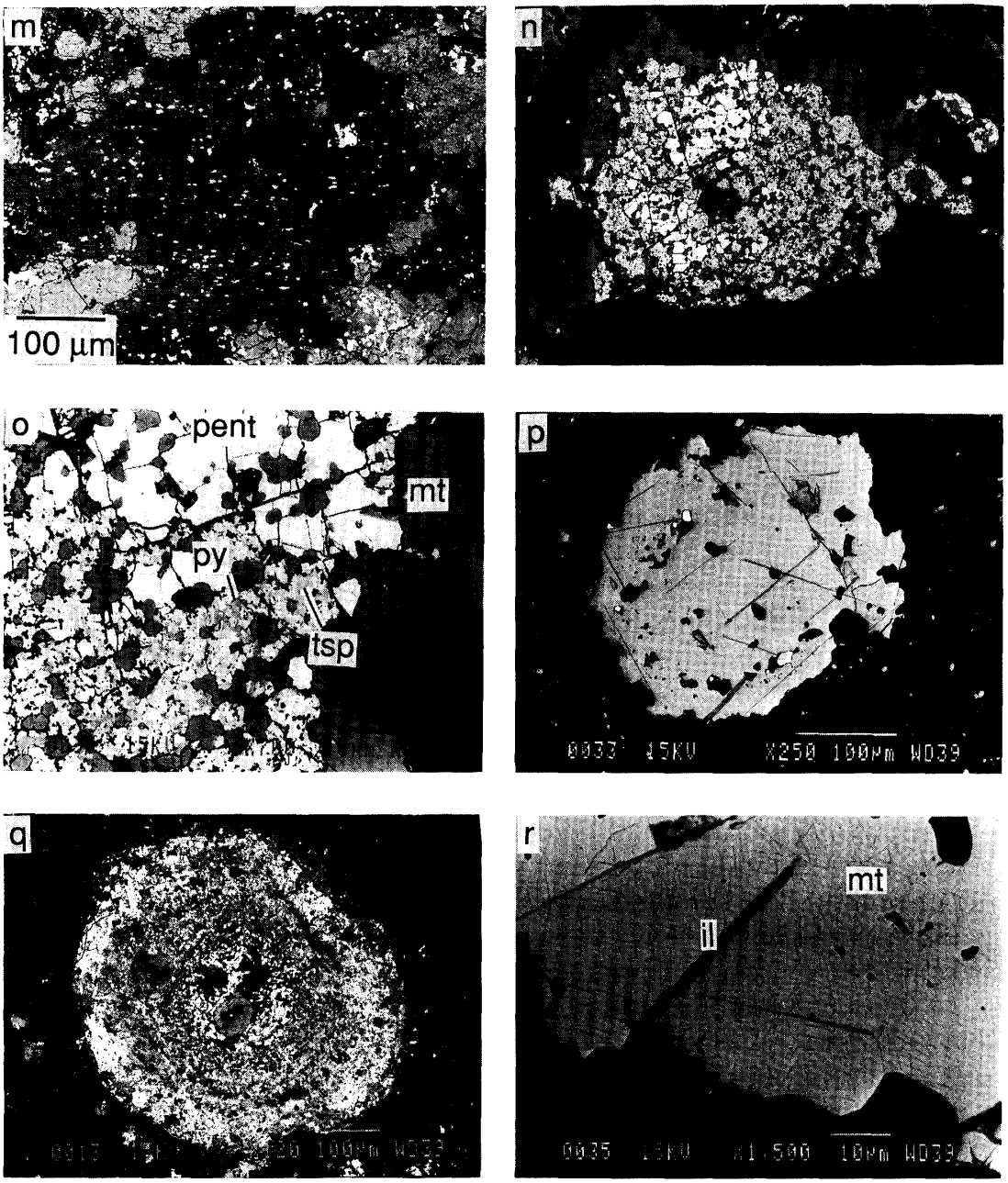

Fig. 1 (Continued).

m. Al-rich low-Ca pyroxene (gray crystal) included in matrix plagioclase (dark) in EET87507. This pyroxene grain includes plagioclase (dark). n. A typical isolated opaque inclusion shown in Y-693. Magnetite (dark) exists on the periphery of the inclusion. o. An enlarged view of Fig. 1n. Fine-grained mixture of pentlandite, pyrite, and thiospinel can be seen. mt: magnetite; pent: pentlandite; py: pyrite; tsp: thiospinel. p. An isolated opaque inclusion in Maralinga. This inclusion is mainly composed of magnetite. Small sulfide inclusions (bright inclusions) and Ca-phosphate inclusions (dark inclusions), and ilmenite lamellae can be observed in the inclusion. q. An isolated opaque inclusion in Karoonda. This inclusion is a fine-grained aggregate of magnetite, pentlandite and pyrite, and displays a concentric structure. r. An enlarged view of an isolated opaque inclusion in Maralinga. Magnetite includes coarse ilmenite lamellae (including tiny spinel inclusions) and thin exsolution lamellae (perhaps spinel).

BISCHOFF, 1990). Most of the large magnetites occur as inclusions with sulfide minerals. In this paper, these inclusions are called isolated opaque inclusions. In the isolated opaque inclusions, the main constituting minerals are the following: magnetite, pentlandite, pyrite, and thiospinel (M_3S_4; M: metal; S: sulfur). In addition to these minerals, chalcopyrite, millerite, and monosulfide were observed in Karoonda, Maralinga, and EET87507, respectively. The principal assemblage of sulfide minerals in CK chondrites has been regarded as pentlandite, pyrite, and monosulfide solid solution (mss) (*e.g.*, GEIGER and BISCHOFF, 1990, 1991b); however, it is clear that the dominant assemblage is magnetite, pentlandite, pyrite, and thiospinel.

Although the principal minerals in the opaque mineral inclusions are the same among these four chondrites, the inclusions in each meteorite show various textures, and the abundances of these minerals in each are various. Grain sizes of the isolated inclusions are from ~ 100 to $\sim 500\,\mu$m. Figure 1n shows a typical type of the opaque mineral inclusions. They are common in three CK chondrites except for Maralinga. Inclusions of this type display a core-rim structure (Fig. 1o). Cores of the inclusions consist of mainly sulfides with a small amount of magnetite. Rims of the inclusions consist of mainly magnetite. In this figure, pentlandite, pyrite and thiospinel show fine-grained intergrowth texture. In some opaque inclusions, they display myrmekitic intergrowth texture. And some inclusions in Karoonda contain chalcopyrite in addition to these minerals. Grain sizes of these minerals in the inclusions are various among the inclusions. In EET87507, however, their sizes ($<5\,\mu$m across) are much smaller than those in other three chondrites.

A typical occurrence of the opaque mineral inclusions in Maralinga is shown in Fig. 1p. This type of inclusion is also observed in EET87507. It is composed mainly of magnetite. Sulfide minerals, Ca-phosphate, and olivine occur as small ($\sim 10\,\mu$m in diameter) inclusions. In some sulfide inclusions in magnetites, millerite coexisting pyrite was observed. Sulfide inclusions in magnetites in EET87507 are larger than those in Maralinga but composed of finer grained sulfides than in Maralinga.

There is another type of opaque mineral inclusion that is shown only in Karoonda (Fig. 1q). This type of inclusion has a concentric structure. In these inclusions, the ratio of magnetite to sulfides decreases as one goes outwards. Olivine was observed at the center. RUBIN (1992) also observed similar objects in EET90007 and ALH82500.

Magnetite in the opaque mineral inclusions has exsolution lamellae and inclusions of ilmenite and spinel. Ilmenite occurs as exsolution lamellae, and the exsolution lamellae include inclusions of spinel (*e.g.*, GEIGER and BISCHOFF, 1990). Most of the spinel inclusions are too fine to analyze by EPMA. Thickness of the ilmenite exsolution lamellae varies from <1 to $10\,\mu$m thick. Magnetite in Maralinga contains two generations of exsolution lamellae (Fig. 1r). Thick lamellae are ilmenite including spinel inclusions. These thin lamellae may be spinel, because EPMA analyses of magnetite including these fine lamellae show <0.5 wt% TiO_2, 4–7 wt% Cr_2O_3 and 1.5–3 wt% Al_2O_3.

3.2. Mineralogy

3.2.1. Olivine

Table 1 shows the average compositions and standard deviations (1σ) of olivines in Karoonda, Maralinga, Y-693, and EET87507. Chemical composition of olivine in

Table 1. Average compositions of olivine in Karoonda, Maralinga, Y-693, and EET87507.

	Karoonda	Maralinga	Y-693	EET87507
	olivine average s.d.	olivine average s.d.	olivine average s.d.	olivine average s.d.
SiO_2	37.46±0.82	36.90±0.32	37.57±0.36	37.12±0.24
TiO_2	0.00±0.01	0.01±0.03	0.00±0.00	0.01±0.02
Al_2O_3	0.02±0.05	0.01±0.02	0.01±0.01	0.03±0.02
Cr_2O_3	0.00±0.04	0.01±0.04	0.00±0.00	0.02±0.02
FeO	26.44±3.51	29.59±0.43	26.57±0.52	26.60±0.41
NiO	0.51±0.16	0.60±0.12	0.41±0.10	0.46±0.09
MnO	0.18±0.07	0.17±0.07	0.24±0.08	0.26±0.04
MgO	35.13±2.97	32.56±0.37	35.05±0.39	34.90±0.37
CaO	0.04±0.13	0.05±0.08	0.02±0.08	0.02±0.05
Na_2O	0.02±0.03	0.00±0.02	0.01±0.03	0.00±0.01
K_2O	0.01±0.01	0.00±0.01	0.00±0.01	0.00±0.01
Total	99.81±0.48	99.89±0.55	99.87±0.71	99.42±0.41
Fo	70.23±4.20	66.24±0.45	70.16±0.46	70.04±0.48

Maralinga, Y-693, and EET87507 is homogeneous, but rather heterogeneous in Karoonda. Some isolated olivine inclusions and olivine oikocrysts enclosed in low-Ca pyroxenes show normal zoning. Their core compositions are from Fo_{80} to Fo_{95}.

Average Fo contents in Karoonda, Y-693, and EET87507 display similar values, around Fo_{70}. On the other hand, olivines in Maralinga are more ferrous, and their average composition is $Fo_{66.2}$. Average CaO contents are from 0.02 to 0.04 wt%; these values are as small as those in equilibrated ordinary chondrites. Average NiO contents are high, ranging from 0.41 to 0.60 wt%. Olivines in Maralinga have the highest average NiO content among these chondrites. These data are consistent with those of previous workers (*e.g.*, SCOTT and TAYLOR, 1985; GEIGER and BISCHOFF, 1991; KELLAR *et al.*, 1992). Average MnO contents are from 0.18 to 0.26. These values are lower than those in olivine with similar Fo contents ($Fo_{69} \sim Fo_{72}$) in equilibrated LL chondrites (LL5 and 6: 0.40–0.46 MnO wt%) (HEYSE, 1981; MCCOY *et al.*, 1991).

3.2.2. Pyroxene

In Fig. 2, pyroxene quadrilaterals illustrate compositions of pyroxenes in these chondrites. This figure shows that pyroxenes in Karoonda are heterogeneous, and that those in other chondrites are more homogeneous than pyroxenes in ordinary chondrites belonging to the same petrologic types.

The average compositions and standard deviations (1σ) of pyroxenes in Karoonda, Maralinga, Y-693, and EET87507 are shown in Table 2. Mean values of minor elements in low-Ca pyroxenes in equilibrated CK chondrites (Maralinga, Y-693, and EET87507) are different from those in low-Ca pyroxenes with similar Fs contents (Fs_{23}–Fs_{26}) in equilibrated LL chondrites. Mean TiO_2 and Cr_2O_3 contents (<0.1 and <0.15 wt%, respectively) are lower than those in equilibrated LL chondrites (LL5 and 6: 0.10–0.25, and 0.09–0.23 wt%, respectively) (HEYSE, 1981; MCCOY *et al.*, 1991). Low TiO_2 and Cr_2O_3 contents in low-Ca pyroxenes in CK chondrites may have resulted from the ubiquitous existence of Cr-bearing magnetite with exsolution lamellae of ilmenite. Mean

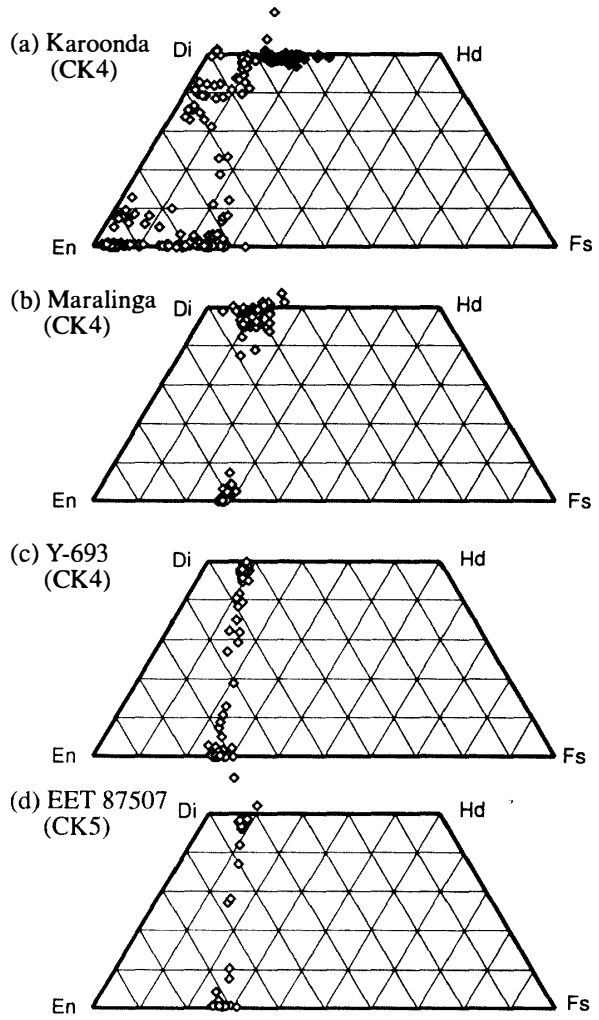

Fig. 2. Pyroxene compositions in Karoonda, Maralinga, Y-693, and EET87507. Filled symbols in Fig. 2a are Fs-rich augites in matrix.

Al_2O_3 contents (0.7–3.45 wt%) are higher than that in the LL chondrites (0.17–0.20 wt%). These high Al_2O_3 contents result from low-Ca pyroxenes in the matrix having high Al_2O_3 contents. Average MnO contents (0.19–0.23 wt%) are lower than those in the LL chondrites (0.39–0.46 wt%). Average CaO contents (0.58–1.04 wt%) are similar to that in the LL chondrites (0.61–1.20 wt%).

The average compositions of augite show the similar tendency to the case of low-Ca pyroxenes. Mean TiO_2, and Cr_2O_3 contents (0.06–0.32 and 0.01–0.08, respectively) tend to be lower than those in augite with similar Fs contents ($Fs_8 \sim Fs_{11}$) in the equilibrated LL chondrites (0.23–0.42, 0.59–0.86, respectively) (HEYSE, 1981). Mean MnO contents (0.19–0.24 wt%) overlap those in the equilibrated LL chondrites (0.13–0.22 wt%). Mean Al_2O_3 contents (1.83–2.58 wt%) are higher than those in equilibrated LL chondrites (0.48–0.61). Mean Na_2O contents (0.17–0.23 wt%) are lower than those in the equilibrated LL chondrites (0.48–0.61 wt%), but higher than those in other carbonaceous chondrits (NOGUCHI, 1989).

As described in the Section 3.1.4, Fs-rich augites are included in the matrix and interstices of microphenocrysts in chondrules in Karoonda. Fs-rich augites in both occurrences contain negligible amounts of non-quadrilateral components. These augites

Table 2. Average compositions of pyroxenes in Karoonda, Maralinga, Y-693, and EET87507.

	Karoonda		Maralinga		Y-693		EET87507	
	Ca-px average s.d.	low-Ca px average s.d.	Ca-px average s.d.	low-Ca px average s.d.	Ca-px average s.d.	low-Ca px average s.d.	Ca-px average s.d.	low-Ca px average s.d.
SiO_2	52.70±1.06	55.35±2.70	52.35±2.12	54.18±0.69	52.81±0.74	53.64±1.33	52.18± 2.69	51.85±1.44
TiO_2	0.34±0.51	0.10±0.15	0.32±0.65	0.01±0.03	0.06±0.07	0.00±0.00	0.27± 0.76	0.02±0.02
Al_2O_3	1.66±1.64	1.56±1.68	1.83±1.89	0.70±0.50	1.98±0.77	2.23±1.67	2.58± 3.92	3.45±1.47
Cr_2O_3	0.35±0.70	0.27±0.26	0.18±0.35	0.03±0.06	0.01±0.03	0.02±0.08	0.13± 0.10	0.14±0.08
FeO	6.65±3.83	11.01±6.06	6.44±1.00	18.01±0.44	6.35±1.41	16.63±0.99	6.74± 3.66	17.22±0.75
NiO	0.07±0.12	0.10±0.10	0.11±0.08	0.16±0.08	0.12±0.13	0.11±0.07	0.09± 0.06	0.13±0.04
MnO	0.13±0.30	0.14±0.10	0.04±0.05	0.19±0.06	0.11±0.07	0.24±0.07	0.11± 0.05	0.23±0.03
MgO	15.47±3.39	30.33±4.47	15.08±1.09	25.83±0.61	16.21±1.42	25.85±1.15	16.93± 3.22	25.49±0.77
CaO	22.31±3.18	1.02±1.55	23.19±0.89	0.72±0.75	21.88±2.88	1.04±1.89	20.59± 6.62	0.58±0.87
Na_2O	0.17±0.19	0.02±0.04	0.23±0.10	0.01±0.02	0.17±0.13	0.02±0.04	0.18± 0.14	0.00±0.00
K_2O	0.00±0.01	0.01±0.01	0.00±0.01	0.01±0.02	0.00±0.01	0.00±0.01	0.00± 0.01	0.00±0.01
Total	99.86±0.57	99.91±0.55	99.77±0.54	99.86±0.55	99.70±0.48	99.78±0.50	99.79± 0.50	99.12±0.51
Wo	45.48±6.21	1.99±3.06	47.15±1.78	1.43±1.47	44.31±5.90	2.08±3.75	41.86±13.84	1.18±1.76
En	43.92±9.70	81.18±9.11	42.60±2.22	70.85±1.41	45.65±3.83	71.95±2.67	47.57± 8.28	71.65±1.56
Fs	10.60±6.10	16.83±9.35	10.25±1.76	27.72±0.69	10.04±2.21	25.98±1.74	10.57± 5.72	27.17±1.45

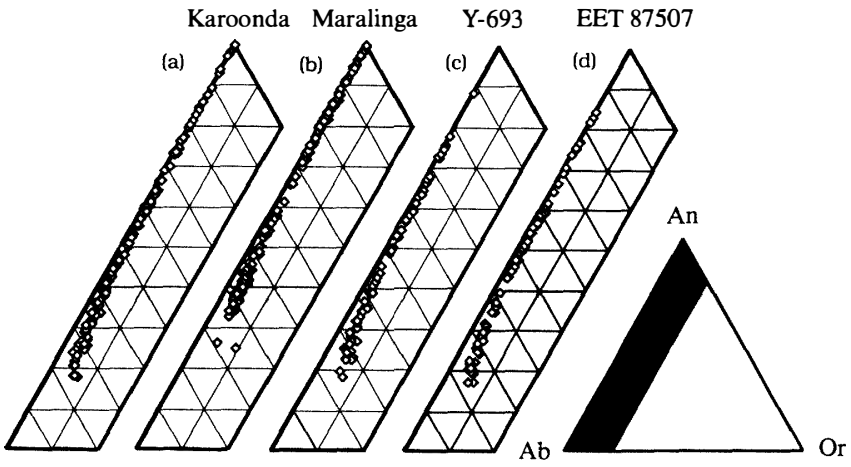

Fig. 3. Plagioclase compositions in Karoonda, Maralinga, Y-693, and EET87507.

are plotted along the join Di and Hd (Fig. 2a). Such augites often show complex zoning of Fs content. Fs-rich augites with similar compositions are observed in the matrix and interstices of microphenocrysts in chondrules in Allende (Kimura, personal communication). Probably Karoonda preserves primary minerals in some degree after metamorphism.

3.2.3. Plagioclase

As described in previous works (*e.g.*, SCOTT and TAYLOR, 1985; GEIGER and BISCHOFF, 1991b), plagioclase compositions are heterogeneous in CK chondrites: Karoonda: $An_{17.9-100}$; Maralinga: $An_{24.9-100}$; Y-693: $An_{18.2-88.5}$; EET87507: $An_{17.4-84.6}$ (Fig. 3). Feldspar with a high Or component was not found in these meteorites.

There are textural differences among plagioclases in chondrules, CAIs, and matrices. Although plagioclases in each occurrence show a wide range of mol% An, they have different compositional variations. Because a small amount of the Or component is included in plagioclases, histograms of mol% An are plotted for plagioclases in the above three occurrences (Figs. 4 to 6).

The proportion of plagioclases with $>An_{80}$ to whole plagioclases is higher than that in matrices (Figs. 4 and 6). Plagioclases in chondrules in Karoonda do not have any peaks on the histogram (Fig. 4a). On the other hand, plagioclases in chondrules in Maralinga show a bimodal distribution (Fig. 4b). The anorthite-rich group has a peak around $An_{90} \sim An_{95}$, and the An-poor group has a peak around $An_{35} \sim An_{40}$. The latter peak corresponds to a peak in the histogram of matrix plagioclases. Plagioclase compositions are different among chondrules in these chondrites. Along with this compositional variation among chondrules, An-rich plagioclases show decrease of An content towards their rims in Maralinga. Analyses of plagioclases in chondrules are few in Y-693 and EET87507, because there are not many chondrules in these chondrites.

Only Maralinga contains many CAIs among the CK chondrites investigated. Plagioclase in CAIs has two peaks around $An_{95} \sim An_{100}$ and $An_{40} \sim An_{45}$ in Maralinga (Fig. 5b). The former peak corresponds to the compositions of plagioclase cores. Anorthite contents decrease at the peripheries of plagioclase crystals, and the latter peak corresponds to the compositions of plagioclase rims. In Karoonda, the mol% An

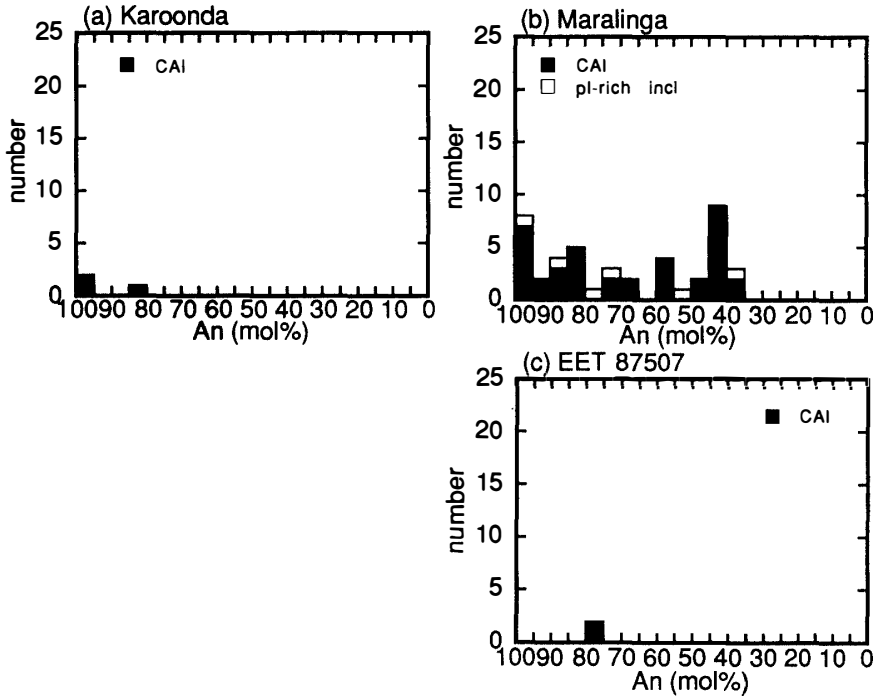

Fig. 4. Histograms of An mol% of plagioclases in CAIs and plagioclase-rich inclusions.

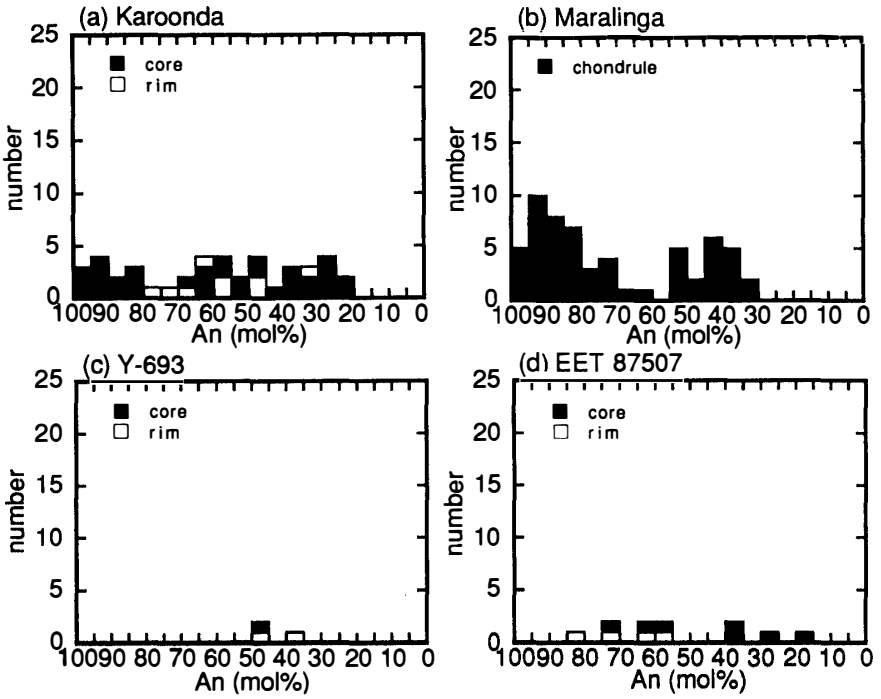

Fig. 5. Histograms of An mol% of plagioclases in chondrules in Karoonda, Maralinga, Y-693, and EET87507.

of plagioclases in CAIs is higher than An_{80} (Fig. 5a). In EET87507, plagioclases in CAIs contain a fairly amount of Ab component (Fig. 5c).

Histograms of An mol% of plagioclases in matrices clearly show that many matrix

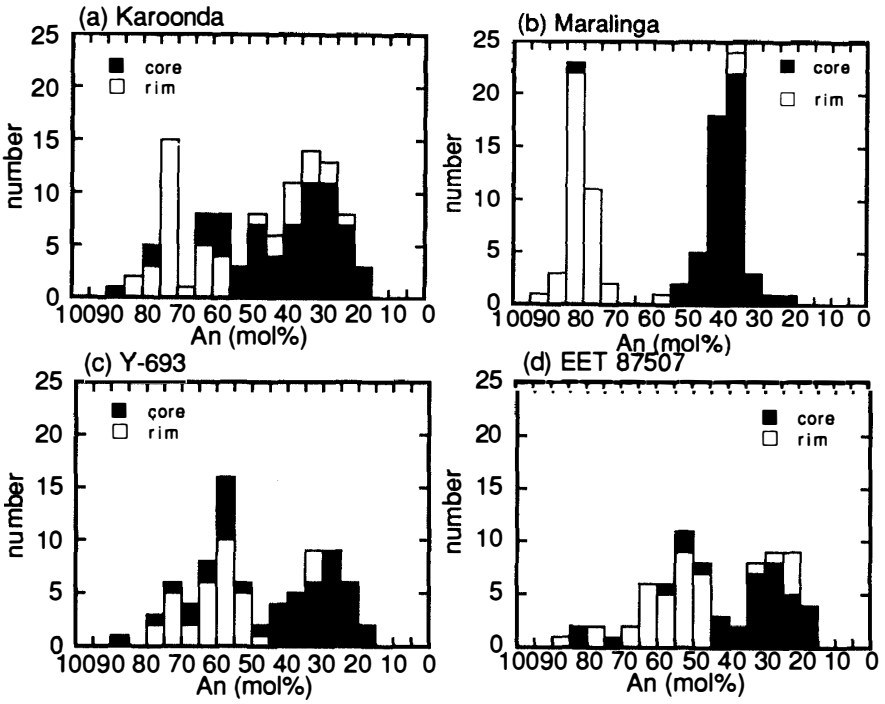

Fig. 6. Histograms of An mol% of plagioclases in matrices in Karoonda, Maralinga, Y-693, and EET87507. These histograms show the reverse zoning of matrix plagioclases.

plagioclases show reverse zoning (Fig. 6). In Maralinga, there is almost no overlap between core and rim compositions of plagioclase (Fig. 6b). This result is consistent with that of KELLER *et al.* (1992) that there are two distinct compositional groups with $\sim An_{20}$ and $\sim An_{80}$, respectively. Although matrix plagioclases in the other three chondrites also show reverse zoning, they do not have sharp peaks, and there are overlaps between core and rim compositions (Figs. 6a, c, and d). Peaks of both core and rim compositions in these three chondrites have lower An contents than those in Maralinga. In addition, compositional ranges of matrix plagioclase in them shift to lower An contents in comparison with those in Maralinga. Among the three chondrites, there is a tendency that peak composition in more recrystallized chondrites shows lower An contents than that in less recrystallized chondrites.

3.2.4. Oxides

Table 3 shows representative analyses of magnetite and ilmenite. DELANEY and MACPHERSON (1987) and KELLER *et al.* (1992) described magnetites in CK chondrites that contain Al_2O_3 and Cr_2O_3. Most of the magnetites in CK chondrites except for Maralinga contain <0.2 wt% TiO_2.; Al_2O_3 and Cr_2O_3 wt% in the magnetites vary from <0.1 to 3 and from 2.5 to 4.5, respectively. On the contrary, TiO_2, Al_2O_3 and Cr_2O_3 contents in magnetites in Maralinga are higher than those in the others: 0.1–0.5, 1.5–3, and 4–7 wt%, respectively. Fine exsolution lamellae ($<1\,\mu$m thick) could not be found in magnetites in CK chondrites by SEM observation except for Maralinga. Therefore, it is not clear whether these oxides were dissolved in magnetites in significant amounts. Because ilmenites in CK chondrites include fine spinel inclusions (GEIGER and BISCHOFF, 1989), fairly high amounts of Al_2O_3 and Cr_2O_3 ($<$ several wt%) were detected

Table 3. Representative analyses of ilmenite and magnetite in Karoonda, Maralinga, Y-693, and EET87507.

	Karoonda	Maralinga		Y-693		EET87507	
mineral	op agg mt	PO il	isl m mt	mtx il	PO mt	op agg il	op agg mt
SiO_2	0.00	0.00	0.00	0.00	0.01	0.02	0.05
TiO_2	0.03	51.80	0.35	50.66	0.00	52.77	0.21
Al_2O_3	2.38	0.00	1.98	0.73	0.27	0.01	0.88
Cr_2O_3	4.74	0.00	5.06	0.46	3.73	0.24	4.41
V_2O_3	0.00	0.00	0.09	0.00	0.00	0.00	0.11
Fe_2O_3	60.88	4.02	60.77	4.49	64.88	1.46	62.92
FeO	30.82	42.17	30.94	41.00	30.63	43.62	31.37
NiO	0.28	0.73	0.50	0.00	0.32	0.19	0.26
MnO	0.00	0.53	0.00	0.86	0.07	0.51	0.03
MgO	0.15	1.78	0.23	1.93	0.09	1.73	0.15
CaO	0.00	0.00	0.00	0.19	0.00	0.06	0.03
ZnO	0.00	0.00	0.00	0.00	0.00	0.00	0.00
Na_2O	0.00	0.00	0.00	0.00	0.00	0.00	0.00
K_2O	0.00	0.00	0.04	0.00	0.00	0.00	0.00
Total	99.28	101.03	99.96	100.32	100.00	100.60	100.43

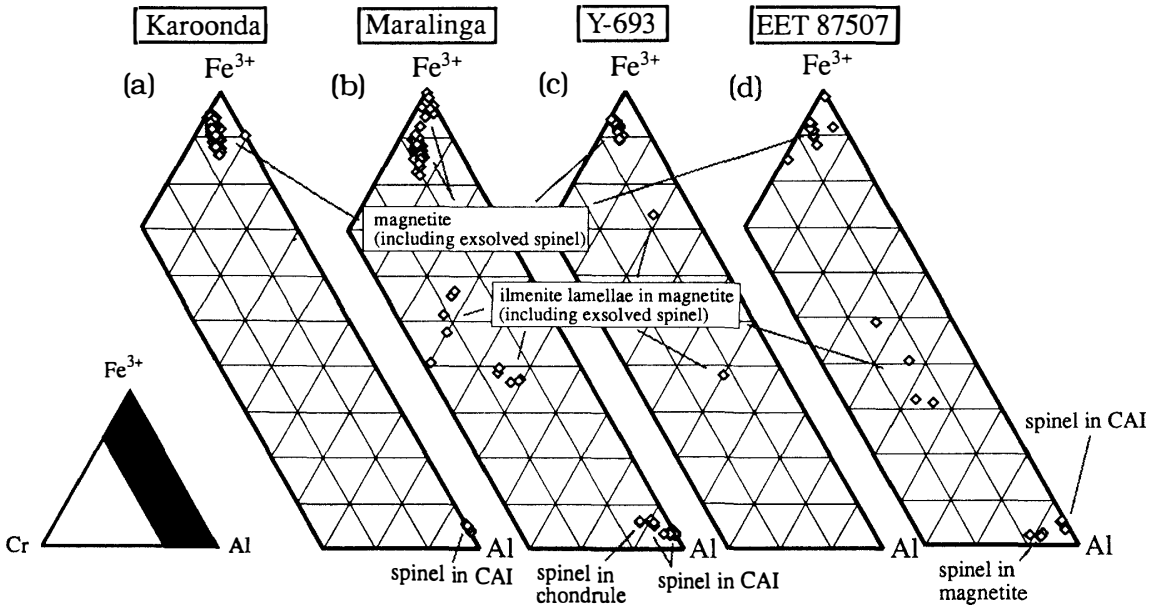

Fig. 7. Cr-Al-Fe^{3+} diagrams of oxides in Karoonda, Maralinga, Y-693, and EET87507.

in ilmenites.

Figure 7 shows Cr-Al-Fe^{3+} diagrams of oxides in CK chondrites investigated. Magnetites in Maralinga form two clusters (Fig. 7b). Magnetites which contain fairly high amounts of Al_2O_3 and Cr_2O_3 occur in matrix and chondrules. Their compositions are similar to those of magnetites in the same occurrences in the other three meteorites. Because magnetites in CAIs include a few spinel lamellae, they are plotted near the

Table 4. Average and representative compositions of spinel in Karoonda, Maralinga, and EET87507, and representative compositions of garnet in Karoonda.

	Karoonda		Maralinga			EET87507			Karoonda	
mineral	CAI sp aver	s.d.	CAI sp aver	s.d.	PO sp	CAI sp aver	s.d.	op agg sp aver	s.d.	CAI gar	CAI gar
SiO_2	0.08±0.15		0.02±0.05		0.00	0.00±0.00		0.00±0.00		40.14	39.01
TiO_2	0.05±0.05		0.01±0.03		0.00	0.00±0.00		0.11±0.04		0.95	0.00
Al_2O_3	59.69±0.78		58.96±1.97		53.75	59.60±0.68		55.53±1.22		20.21	22.24
Cr_2O_3	0.02±0.03		1.19±1.17		5.27	0.72±0.06		6.48±0.98		0.00	0.00
V_2O_3	0.02±0.05		0.01±0.02		0.00	0.00±0.00		0.00±0.00		0.01	0.00
Fe_2O_3	4.82±0.58		4.30±0.94		5.59	4.53±0.79		2.06±0.15		3.17	0.87
FeO	19.86±0.65		21.68±0.72		24.52	19.63±0.33		21.62±0.76		0.46	0.00
NiO	1.08±0.11		1.13±0.16		1.08	1.00±0.10		0.44±0.11		0.08	0.02
MnO	0.03±0.02		0.08±0.06		0.00	0.06±0.05		0.03±0.04		0.00	0.00
MgO	12.58±0.36		11.45±0.53		9.31	12.46±0.23		10.77±0.42		8.61	0.00
CaO	0.15±0.20		0.07±0.07		0.00	0.04±0.04		0.00±0.01		25.81	37.87
ZnO	1.14±0.38		0.86±0.49		0.84	1.59±0.12		2.24±0.23		0.00	0.00
Na_2O	0.00±0.00		0.00±0.01		0.00	0.01±0.01		0.00±0.00		0.00	0.00
K_2O	0.01±0.02		0.01±0.02		0.00	0.01±0.01		0.02±0.02		0.00	0.00
Total	99.52±0.44		99.77±0.48		100.36	99.66±0.31		99.31±0.09		99.44	100.01

Fe^{3+} apex. Because ilmenites exist as isolated crystals in CAIs (*e.g.*, KELLER, 1992), TiO_2 contents in the magnetites are lower than those in magnetites in the other occurrences.

Spinels in CK chondrites were observed as one of the major phases in CAIs, inclusions in magnetites, and rarely as an accessory phase in a chondrule. They are Al-rich spinel (pleonaste), and contain fairly amounts of Cr_2O_3, NiO, and ZnO: <0.1–6.5, 0.4–1.1, and 0.8–2.3 wt%, respectively (Table 4).

Spinels in different occurrences have different chemical compositions. Cr_2O_3 contents in spinels in CAIs are lower than those in chondrules and in magnetites (Fig. 7). Although chromites are often included in type II chondrules in other C chondrites (MCCOY *et al.*, 1991), no chromite was observed in CK chondrites. This observation may be related to the ubiquitous existence of Cr-bearing magnetite in CK chondrites. MACPHERSON and DELANEY (1985) and KELLER *et al.* (1992) reported compositions of spinel in CAIs in Karoonda and Maralinga. Their results also show that Cr_2O_3 contents in Karoonda are lower than that in Maralinga.

ZnO contents in spinels are similar to NiO contents. In EET87507, spinels in magnetites contain >2 wt% ZnO. YABUKI *et al.* (1983) reported that pleonaste-rich spinels in chondrules in L and LL chondrites contain up to 2.3 wt% ZnO. They suggested that precursor materials of chondrules contained both refractory (Al) and volatile (Zn) elements. In CK chondrites, however, spinels in various objects such as CAIs, chondrules, and magnetites contain fairly high amounts of ZnO. Therefore, in the case of CK chondrites, it may be plausible that a high ZnO content in spinel is related to metamorphism which CK chondrites experienced.

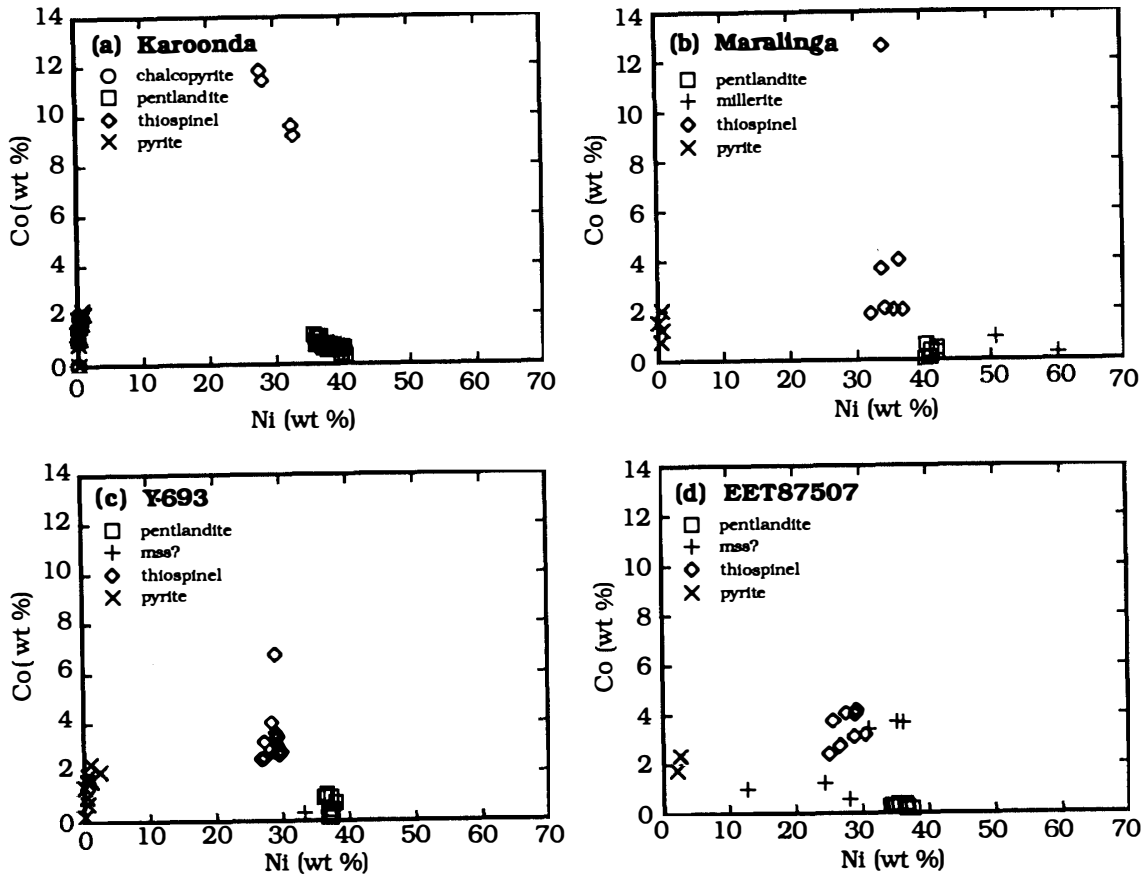

Fig. 8. Plots of Ni vs. Co wt% in sulfide minerals in Karoonda, Maralinga, Y-693, and EET87507.

Spinel compositions suggest that they contain Fe_2O_3. Because fine magnetites in spinels (KELLER *et al.*, 1992) were carefully avoided, such analyses do not result from the contamination from the magnetites. Ferric-ferrous ratios in each chondrites show similar values (~ 0.2).

3.2.5. Sulfides

As described in Section 3.1.4, opaque mineral inclusions contain sulfides. Table 4 displays average compositions of sulfides. SCOTT and TAYLOR (1985) reported chalcopyrite from Karoonda and PCA82500. In this study, chalcopyrite was not observed in studied meteorites except for Karoonda. Chalcopyrite does not contain Co, although other sulfides contain Co in fairly high amounts.

Each sulfide contains different amounts of Co and Ni (Fig. 8). The Co contents in the three major sulfide minerals increase in the following order: pentlandite, pyrite, thiospinel . Some thiospinels contain Co, up to ~ 13 wt%. The thiospinels in CK chondrites are violarite $FeNi_2S_4$ in which Co replaces Ni (Table 5 and Fig. 9).

Figure 8 shows coexisting sulfide minerals in each meteorite. Pentlandite, pyrite, and thiospinel coexist in all the meteorites investigated. In addition to these minerals, it was observed that millerite NiS coexists with pyrite in Maralinga. There seems to be monosulfide(s) in EET87507.

The coexistence of pentlandite, pyrite, and thiospinel, and that of pyrite and millerite

Table 5. Average compositions of sulfides in Karoonda, Maralinga, Y-693, and EET87507.

	Karoonda				Maralinga			
mineral	cp	pent	thiosp	py	pent	ml	thiosp	py
	aver s.d.	aver s.d.	aver s.d.	aver s.d.	aver s.d.	aver s.d.	aver s.d.	aver s.d.
S	35.25±0.15	33.57±0.38	42.45±0.66	53.22±0.42	33.03±0.31	34.81±0.03	42.42±0.40	53.38±0.61
Fe	30.15±0.94	26.73±1.31	15.67±1.86	44.80±0.76	25.31±0.81	8.81±6.43	17.94±3.69	44.94±0.19
Co	0.03±0.03	1.09±0.18	10.42±1.31	1.49±0.48	0.28±0.21	0.58±0.42	4.16±3.90	1.40±0.53
Ni	0.12±0.10	37.68±1.43	30.34±2.69	0.33±0.26	41.01±0.67	55.41±6.53	35.08±1.64	0.44±0.28
Cu	32.10±0.69	0.00±0.00	0.00±0.00	0.03±0.05	0.00±0.00	0.00±0.00	0.00±0.00	0.09±0.11
Total wt	97.67±0.27	99.08±0.48	98.89±0.94	99.88±0.59	99.62±0.50	99.61±0.35	99.60±0.68	100.24±0.70

	Y-693				EET87507			
mineral	pent	mss?	thiosp	py	pent	mss?	thiosp	py
	aver s.d.		aver s.d.	aver s.d.	aver s.d.	aver s.d.	aver s.d.	aver s.d.
S	33.29±0.33	36.58	43.30±0.63	53.29±0.55	33.42±0.62	38.31±1.21	42.12±0.49	51.80±0.63
Fe	28.28±0.31	30.58	24.78±1.59	44.52±1.08	29.51±1.02	30.11±9.42	25.28±2.51	42.55±1.26
Co	0.54±0.36	0.34	3.24±1.15	1.47±0.66	0.28±0.07	2.32±1.48	3.55±0.66	2.07±0.42
Ni	37.13±0.45	33.28	28.90±0.97	0.82±0.72	35.84±1.11	28.32±8.62	28.27±1.90	2.54±0.66
Cu	0.00±0.00	0.00	0.00±0.00	0.00±0.00	0.11±0.34	0.02±0.04	0.00±0.00	0.00±0.00
Total wt	99.24±0.35	100.78	99.23±0.54	100.10±0.52	99.17±0.53	99.08±0.85	99.22±0.79	98.96±0.46

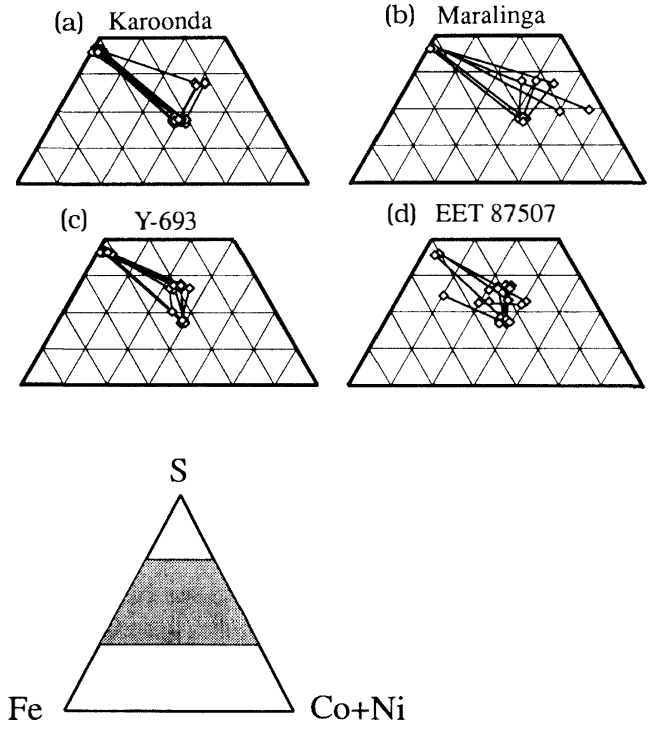

Fig. 9. Fe-(Co+Ni)-S diagrams of Fe-Co-Ni-sulfides in Karoonda, Maralinga, Y-693, and EET87507. The assemblage pentlandite-pyrite-thiospinel (Co-rich violarite) is predominant in these chondrites.

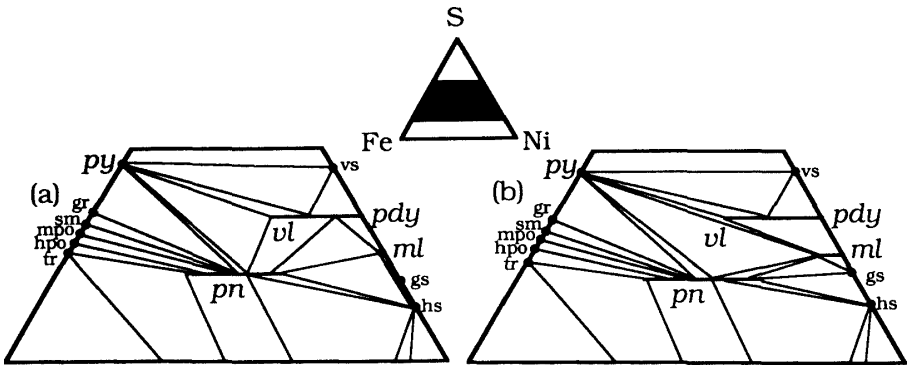

Fig. 10. Schematic alternative interpretations of low-temperature equilibrium in the Fe-Ni-S system after CRAIG and SCOTT (1976).

(Fig. 9) can be interpreted as equilibrium mineral assemblages under low temperatures. CRAIG and SCOTT (1976) showed schematic alternative interpretations of low-temperature equilibrium in the Fe-Ni-S system (Fig. 10). Because pentlandite, pyrite, and thiospinel were observed in all the meteorites investigated, Fig. 10a is more plausible than Fig. 10b. In Maralinga, the assemblage of pyrite and millerite was also observed. This observation can be interpreted in two ways. One interpretation is that the assemblage of pyrite and pentlandite is metastable, and another is that tie lines change from Fig. 10b to Fig. 10a as temperature decreases due to the limited range of solid solution in

millerite. Because grain sizes of sulfides in EET87507 are several μm across at best, the possibility cannot be excluded that observed monosulfides are mixture of pentlandite, pyrite and thiospinel.

Anyway, these assemblages can be formed under low temperatures (perhaps below $\sim$450°C) considering the thermal stability of violarite (461°C; VAUGHAN and CRAIG, 1978). These observations may suggest that CK chondrites were cooled slowly so that the low temperature equilibrium assemblages were formed.

4. Discussion

4.1. Reverse zoninig of matrix plagioclase

It is a problem how these compositionally variable plagioclases were formed. RUBIN (1992) suggested that these plagioclases may have been formed by shock metamorphism. However, compositions, grain sizes, and occurrences of plagioclases in CK chondrites are different from feldspars in ordinary chondrite (OC) breccias. Most of the feldspars in OC breccias have compositional trends from oligoclase to orthoclase (BISCHOFF *et al.*, 1983). An LL7 chondrite, Y-74160, includes plagioclases with significant compositional variation ($An_5 \sim An_{25}$) (TAKEDA *et al.*, 1985), and also includes potassic feldspars. In OC breccias and Y-74160, compositions of feldspars obey the crystallization trend of feldspar: crystallization of plagioclase (calcic→sodic)→cotectic crystallization of sodic plagioclase and K-feldspar. Compositionally variable feldspars in these chondrites resulted from crystallization of them in veins and melt pockets with various compositions. In each vein and melt pocket, feldspar crystallized as described above.

On the other hand, no feldspar grain obeying such a compositional trend was observed in this study (Fig. 3). As described previously, the chemical compositions of plagioclases in CK chondrites are different among matrices, chondrules, and CAIs. Moreover, most of the matrix plagioclases show reverse zoning of An contents, and potassic feldspar was not observed in all the CK chondrites investigated. Apparently, normal crystallization of feldspars which governs compositions of feldspars in the OC breccias and Y-74160 cannot make these plagioclases in CK chondrites.

The textures of plagioclases in CK chondrites are also different from those in the OC breccias and Y-74160. Feldspars in OC breccias occur as anhedral crystals (<a few tens μm across) filling irregular and tenuous veins and melt pockets, and such occurrences are quite different from the occurrences of plagioclase as described in Section 3.1.

In CK chondrites, reverse zoning of matrix plagioclases can be observed, regardless of degree of recrystallization. Therefore, the reverse zoning seems to have been formed during metamorphism. Most of the cores of matrix plagioclase have An contents from An_{20} to An_{40}. Under oxidized conditions, sodic plagioclase ($\sim An_{20}$) can be condensed from the protosolar nebula (WOOD and HASHIMOTO, 1988). There may be a possibility that cores of matrix plagioclase were primarily condensates from the nebula and recrystallized during thermal metamorphism. If abundant nepheline had been condensed and accreted as one of original CK materials, abundant SiO_2 derived from pyroxene would have been consumed to make sodic plagioclase during metamorphism. If abundant matrix plagioclases ($\sim$30 vol% in matrix in Y-693: OKADA, 1975) had been formed by

the reaction between nepheline and SiO_2 derived from pyroxenes, most of pyroxenes would have been used up during metamorphism. In CK chondrites except for Maralinga, however, pyroxenes are included in matrix plagioclases. Therefore, condensation of abundant nepheline is implausible in the history of CK chondrites.

After recrystallization of cores of sodic matrix plagioclase, breakdown of minerals which include Ca, Al, and Si would result in making reverse zoning of matrix plagioclase. Because there is no type 3 CK chondrite at present, we assume tentatively that the minerals in the CK chondrites investigated reacted to form the reverse zoning of plagioclase. One example of the reactions to form reverse zoning of plagioclase from such augite is:

$$\underset{\text{opx}}{2MgSiO_3} + \underset{\text{cpx}}{CaMgSi_2O_6} + \underset{\text{sp}}{MgAl_2O_4} \rightarrow \underset{\text{pl}}{CaAl_2Si_2O_8} + \underset{\text{ol}}{2Mg_2SiO_4}\,. \qquad (1)$$

If this reaction occurred, olivine in the right side of reaction (1) may have equilibrated with primary olivine.

4.2. *Composition of low-Ca pyroxene enclosed in matrix plagioclase*

Most of the pyroxene crystals (both low-Ca pyroxene and augite) in matrices are enclosed in plagioclase in Karoonda, Y-693, and EET87507. They are acicular in shape. In EET87507, some low-Ca pyroxenes include plagioclase inclusions (Fig. 1m) and there is no tabular low-Ca pyroxene crystals as shown in Fig. 1b.

In pyroxene quadrilateral diagrams, matrix pyroxenes have almost the same composition as pyroxenes in chondrules (Fig. 2). However, pyroxenes, especially low-Ca pyroxenes, in matrix plagioclases are plotted in different areas from pyroxenes in chondrules in a plot of Al_2O_3 *vs.* CaO contents (Fig. 11). In this figure, low-Ca pyroxenes in chondrules have a trend in which Al_2O_3 content increases as CaO content increases. On the contrary, low-Ca pyroxenes in the matrix show a trend in which Al_2O_3 content increases but CaO content does not increase, or rather seems to decrease slightly.

Figure 12 shows plots of Al_2O_3 *vs.* CaO (wt%) for low-Ca pyroxenes in matrix

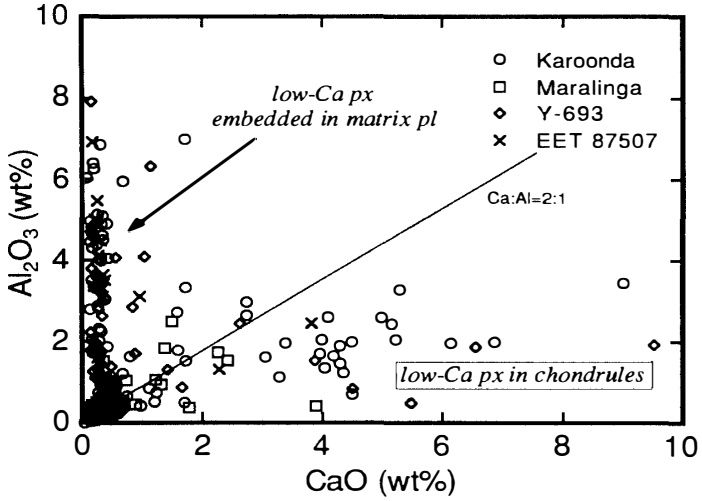

Fig. 11. A plot of CaO and Al_2O_3 wt% of low-Ca pyroxenes in the CK chondrites investigated.

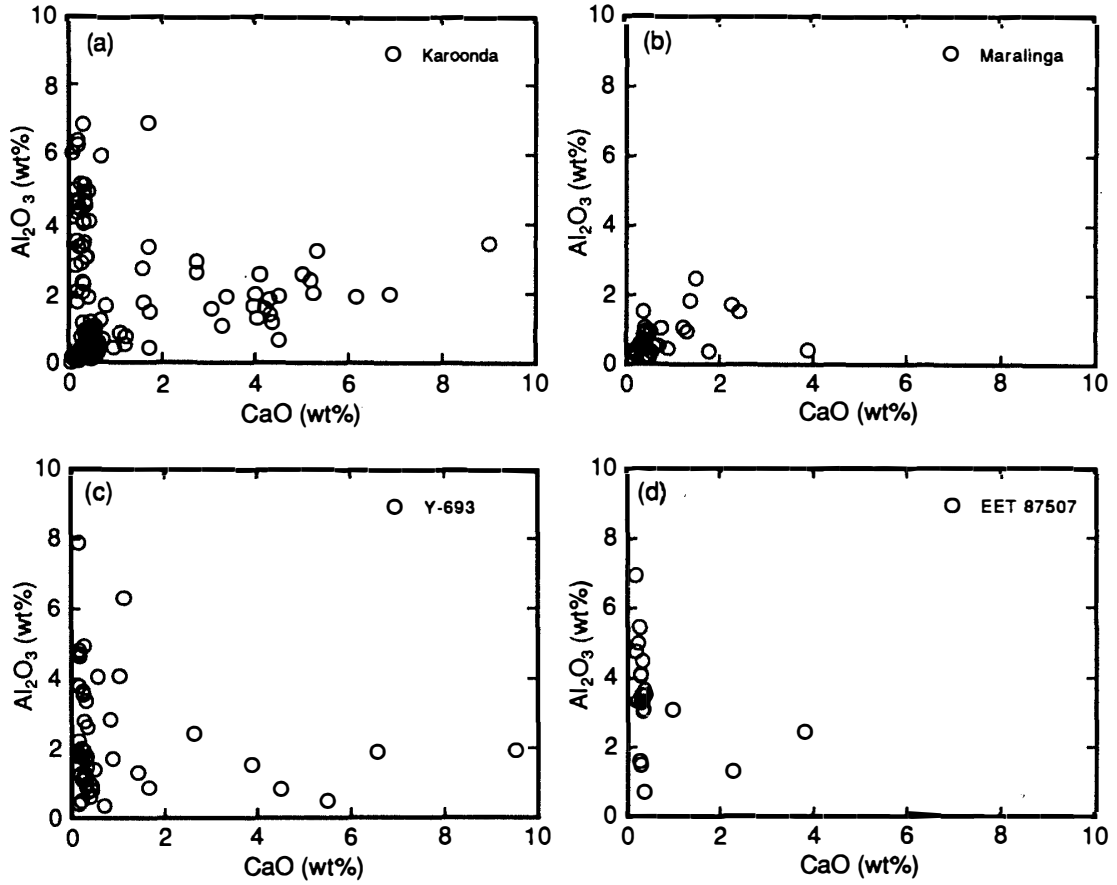

Fig. 12. Plots of CaO and Al_2O_3 wt% of low-Ca pyroxenes in Karoonda, Maralinga, Y-693, and EET87507.

plagioclases in each meteorite. In Karoonda, plagioclases occur in mesostases of chondrules and as a main constituent mineral of fragments which include acicular pyroxenes. Figure 12a clearly shows that there are two trends of low-Ca pyroxenes. Low-Ca pyroxenes in matrix and acicular low-Ca pyroxenes in some chondrules (*e.g.*, Fig. 1c) are plotted on the same trend. Because low-Ca pyroxenes are scarcely observed in the matrix of Maralinga, only a trend of low-Ca pyroxenes in chondrules is observed (Fig. 12b). In Y-693 and EET87507, most of low-Ca pyroxenes are enclosed in matrix plagioclases. Therefore, most of low-Ca pyroxenes in these meteorites are plotted on a trend of low-Ca pyroxenes in matrix.

Figure 13 shows that there is a strong positive correlation ($r=0.84$) between FeO and Al_2O_3 contents for low-Ca pyroxenes in matrix. There is a possibility that these pyroxenes contain Fe^{3+} and that Fe^{3+} and Al are positively correlated. To assess the existence of Fe^{3+} in these pyroxenes, the relationships between 2-Si and $Al+Ti+Cr$-Na and $Al+Ti+Cr+Fe^{3+}$-Na of the low-Ca pyroxenes are plotted (Fig. 14). The Fe^{3+} content is calculated by the assumption that the deficiency of total wt% and excess cations (total cations-4, based on 6 oxygens) are attributed to the existence of Fe^{3+}. Because TiO_2, Cr_2O_3, and Na_2O contents are <0.1 wt% in these pyroxenes, Fig. 14 can be regarded as the relationships between 2-Si and Al, 2-Si and $Al+Fe^{3+}$. This

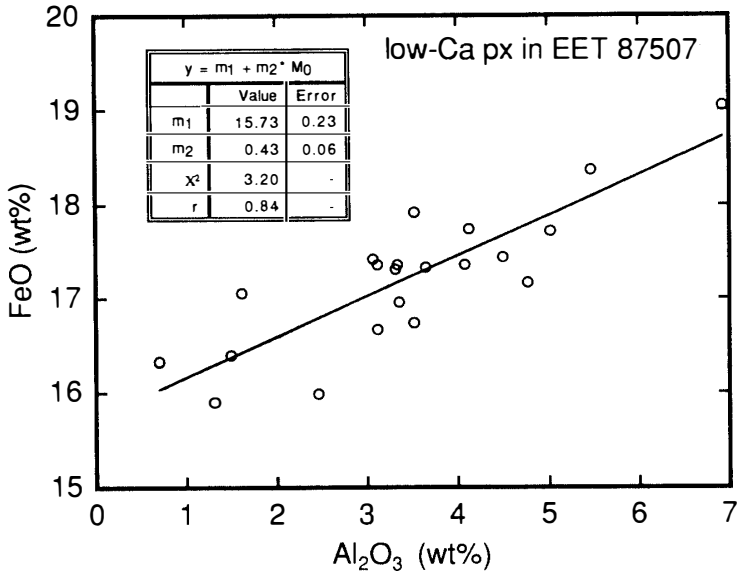

Fig. 13. A plot of Al_2O_3 and FeO wt% in low-Ca pyroxenes in matrix in EET87507. There is a good positive correlation ($r=0.84$) between Al_2O_3 and FeO wt%.

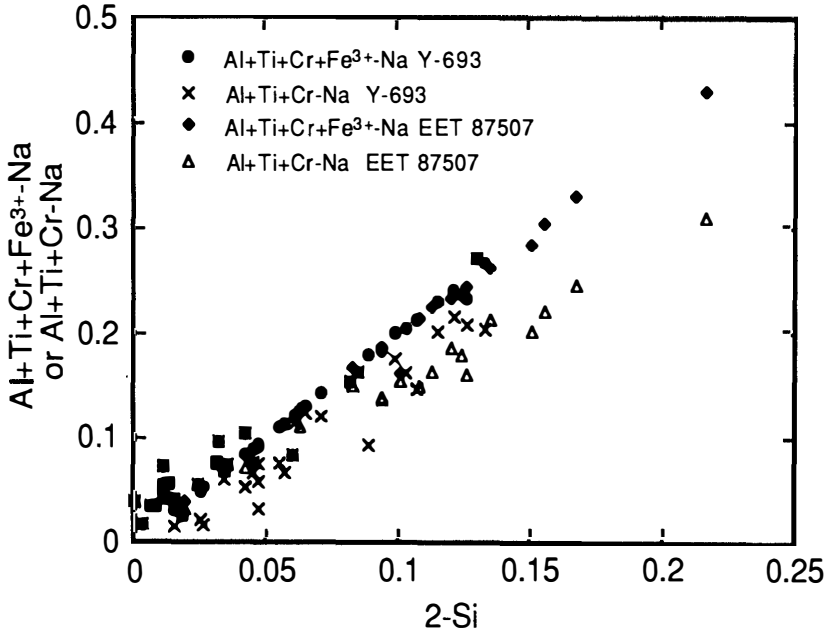

Fig. 14. A composite plot for (2-Si) vs. ($Al+Ti+Cr+Fe^{3+}$) and (2-Si) and ($Al+Ti+Cr+Fe^{3+}$-Na) in low-Ca pyroxenes in matrices in Y-693 and EET87507. Stoichiometry of low-Ca pyroxenes becomes better when Fe^{3+} is considered.

figure shows that there is a positive correlation between 2-Si and Al. And it is clear that stoichiometry of the low-Ca pyroxenes becomes better when the existence of Fe^{3+} is assumed, because pyroxene compositions are plotted along the line with an inclination of 2 in Fig. 14 when stoichiometry of pyroxenes is attained. Therefore, Al_2O_3 and Fe_2O_3 are incorporated in the low-Ca pyroxenes by the substitutions $^{VI}Mg\ ^{IV}Si = {}^{VI}Al\ {}^{IV}Al$ and $^{VI}Mg\ ^{IV}Si = {}^{VI}Fe^{3+}\ {}^{IV}Al$. Figure 14 also indicates that the Fe^{3+} content in the

octahedral site (difference between Al + Ti + Cr-Na and Al + Ti + Cr + Fe^{3+}-Na with the same 2-Si value) increases as Al in the tetrahedral site (2-Si) increases. These data suggest that both $MgAl_2SiO_6$ (MgATs) and $MgFe^{3+}AlSiO_6$ (MgFATs) molecules are incorporated in these low-Ca pyroxenes. However, solubilities of MgATs and MgFATs molecules are very low under low-P conditions (ARIMA, 1978). Probably these molecules were incorporated metastably into the low-Ca pyroxenes during metamorphism.

Due to the absence of type 3 CK chondrite, we assume tentatively that the minerals in the CK chondrites investigated reacted to form the MgATs- and MgFATs-rich low-Ca pyroxene. Two examples of the reactions to form such low-Ca pyroxenes are:

$$\underset{\text{opx}}{4MgSiO_3} + \underset{\text{cpx}}{CaMgSi_2O_6} + \underset{\text{sp}}{2MgAl_2O_4} \rightarrow \underset{\text{pl}}{CaAl_2Si_2O_8} + \underset{\text{MgATs}}{MgAl_2SiO_6} + \underset{\text{ol}}{3Mg_2SiO_4}\,. \quad (2)$$

$$\underset{\text{opx}}{8MgSiO_3} + \underset{\text{px}}{CaMgSi_2O_6} + \underset{\text{sp}}{3MgAl_2O_4} + \underset{\text{mt}}{Fe_3O_4}$$

$$\rightarrow \underset{\text{pl}}{CaAl_2Si_2O_8} + \underset{\text{MgATs}}{MgAl_2SiO_6} + \underset{\text{MgFATs}}{MgFe^{3+}AlSiO_6} + \underset{\text{ol}}{5(Mg_{0.9}Fe_{0.1})_2SiO_4}\,. \quad (3)$$

If these reactions occurred, it may be thought that olivines formed by these reactions attained equilibrium between primary olivines.

4.3. *Metamorphism of CK chondrites*

The olivine-spinel geothermometer suggests that Maralinga, Y-693, EET87507, and some fragments in Karoonda were heated to at least 750 to 850°C (Fig. 15). A spinel in a PO chondrule in Maralinga shows high temperature (> 1200°C). It is not clear whether this spinel records igneous temperatures or not.

GEIGER and BISCHOFF (1991) reported that 650°C was estimated by a two-pyroxene geothermometer for Maralinga. However, pyroxene compositions (Fig. 2) in these studied CK chondrites including Maralinga are definitely more homogeneous than those in ordinary chondrites belonging to the same petrologic types. Therefore, pyroxene quadrilateral compositions also suggest that their peak metamorphic temperatures were as high as those of type 5 to 6 ordinary chondrites. These results mean that even though chondrites belonging to the different chemical groups are classified as the same petrologic

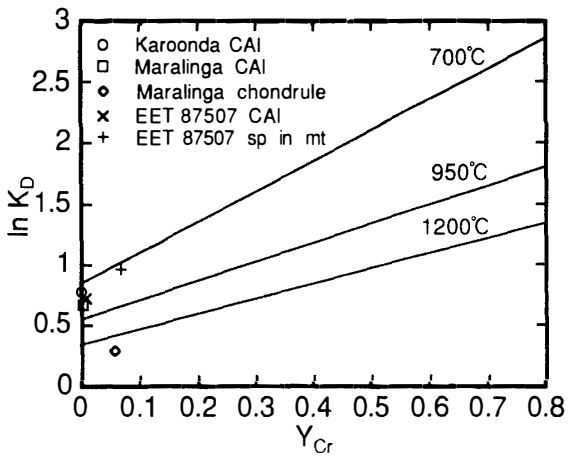

Fig. 15. A plot of Y_{Cr} vs. Fe-Mg distribution coefficient between olivine and spinel. Isotherms are after FABRIÈS (1979).

type, it does not necessarily indicate that they experienced similar thermal histories. In other words, CK4 and 5 chondrites probably experienced higher metamorphic temperatures than other chondrites belonging to the same petrologic type.

Oxygen isotopes of whole rocks, chondrules and minerals in Karoonda and Y-693 were investigated by CLAYTON *et al.* (1977, 1979). Because magnetite, matrix plagioclase, and pyroxene changed (or formed in the case of pyroxene in matrix plagioclase) their compositions during metamorphism, it is reasonable that they are plotted near a fractionation line. Olivine in chondrules show overgrowth of olivine on primary olivine microphenocrysts (Fig. 1a). It may be a reason that olivine in PO chondrules leaves from the Allende mixing line. About 540°C was estimated by CLAYTON *et al.* (1977, 1979) by assuming equilibrium of the three oxygen isotopes among magnetite, plagioclase. However, as discussed above, it is clear that these meteorites were heated to higher temperatures than 540°C. In addition, sulfide mineral assemblages suggest slow cooling (Section 3.2.5). The estimated temperature is apparent and probably related to the blocking temperatures of these minerals during the cooling stage.

At the early stage of metamorphism, grain growth of matrix sodic plagioclases and formation of pyroxenes (especially Al-rich low-Ca pyroxenes) in them probably occurred. And overgrowth of calcic plagioclases (sharp or diffuse) on them probably followed. Zoning patterns of matrix plagioclases were probably due to different thermal history after overgrowth of calcic plagioclase. The assemblages of sulfide minerals were probably accomplished during slow cooling at the late stage of metamorphism. Metamorphism of CK chondrites probably occurred under high oxygen fugacities. This is suggested by the existence of Fe^{3+} in spinel and low-Ca pyroxene. However, it is impossible to estimate oxygen fugacities by a Fe-Ti oxide geothermometer and geobarometer at present, because both precise compositions of them cannot be estimated due to fine spinel inclusions.

4.4. Maralinga as an anomalous CK chondrite

Maralinga has many properties which distinguish this chondrite from other studied CK chondrites. They are: ubiquitous replacement texture of low-Ca pyroxene by olivine in chondrules, very low abundance of low-Ca pyroxene in matrix, abundant CAIs (KELLER *et al.*, 1992a, b), distinct compositions between cores and rims of matrix plagioclases, and peak compositions of both cores and rims being the most An-rich among studied CK chondrites.

Calcium in this meteorite is most abundant among all CK chondrites (KALLEMEYN *et al.*, 1991). This high Ca abundance is probably related to higher abundance of CAIs and higher An contents of matrix plagioclases. These observations suggest that Maralinga is an anomalous CK chondrite, as proposed by KELLER *et al.* (1992a).

5. Conclusions

(1) Plagioclases in chondrules, CAIs, and matrices in CK chondrites show compositional zoning, and those in the matrix show distinct reverse zoning in regard to An content. Cores of matrix plagioclases were perhaps formed by recrystallization of primary plagioclases. Rims of matrix plagioclases were probably formed during

metamorphism.

(2) Low-Ca pyroxenes in chondrules is different in CaO and Al_2O_3 contents from those set in matrix plagioclases. Compositions of low-Ca pyroxenes in matrix plagioclases suggest that they include Fe^{3+}. They were probably formed during metamorphism under high oxygen fugacities. This is suggested by the existence of Fe^{3+} in spinel and low-Ca pyroxene.

(3) Olivine-spinel geothermometry suggests that Maralinga, Y-693, EET87507, and some fragments in Karoonda were heated to at least 750 to 850°C. Pyroxene quadrilateral compositions in these chondrites also suggest that peak metamorphic temperatures were as high as those of type 5 to 6 ordinary chondrites. Slow cooling of these meteorites was estimated by sulfide mineral assemblages.

(4) Maralinga is an anomalous CK chondrite, because Maralinga has many different properties from other CK chondrites investigated. For instance, this meteorite shows replacement textures of low-Ca pyroxene by olivine in chondrules ubiquitously, a very low abundance of low-Ca pyroxene, and abundant CAIs. Moreover, compositions of both cores and rims of maritx plagioclases in this meteorite rarely overlap each other and are the most An-rich among studied CK chondrites.

Acknowledgments

I am grateful to the National Institute of Polar Research, American Museum of Natural History and the Meteorite Working Group of NASA for giving the loan of the meteorite samples. I am also grateful to Drs. Y. IKEDA and M. KIMURA for discussions. Mr. David NEW kindly sold specimens of the Maralinga meteorite to me. Scanning electron microscopy was performed at the Geological Institute, University of Tokyo. Microprobe analyses of EET87507 were performed at the Ocean Research Institute, University of Tokyo. Mr. H. YOSHIDA and Dr. T. ISHII are appreciated for their permission to use the SEM and the EPMA, respectively. Helpful criticisms and suggestions by Drs. M. KITAMURA and A. E. RUBIN are gratefully acknowledged. This work was supported by the Grant-in-Aid for Scientific Research, from the Ministry of Education, Science and Culture, Japan (Nos. 02952114 and 04740451).

References

ARIMA, M. (1978): Phase equilibria in the system $MgSiO_3$–Al_2O_3–Fe_2O_3 at high temperatures and pressures, with special reference to the solubility of Al_2O_3 and Fe_2O_3 in enstatite. J. Fac. Sci., Hokkaido Univ., Ser. IV, **18**, 305–338.

BISCHOFF, A., RUBIN, A. E., KEIL, K. and STÖFFLER, D. (1983): Lithification of gas-rich chondrite regolith breccias by grain boundary and localized shock melting. Earth Planet. Sci. Lett., **66**, 1–10.

BREARLEY, A. J. and SCOTT, E. R. D. (1987): Electron petrography of fine-grained matrix in the Karoonda C4 carbonaceous chondrite. Meteoritics, **22**, 339–340.

CRAIG, J. R. and SCOTT, S. D. (1976): Sulfide phase equilibria. Sulfide Mineralogy, Reviews in Mineralogy, Vol. 1, ed. by P. H. RIBBE. Washington, Mineralogical Society of America, CS1–110.

DELANEY, J. S. and MACPHERSON, G. J. (1987): The Karoonda chondrule corundum conundrum. Lunar and Planetary Science XVIII. Houston, Lunar Planet. Inst., 175–176.

CLAYTON, R. N., Onuma, N., GROSSMAN, L. and MAYEDA, T. K. (1977): Distribution of the pre-solar component in Allende and other carbonaceous chondrites. Earth Planet. Sci. Lett., **34**, 209–224.

CLAYTON, R. N., MAYEDA, T. K. and ONUMA, N. (1979): Oxygen isotopic compositions of some Antarctic meteorites. Lunar and Planetary Science X. Houston, Lunar Planet. Inst., 221–223.

FABRIÈS, J. (1979): Spinel-olivine geothermometry in peridotites from ultramafic complexes. Contrib. Mineral. Petrol., **69**, 329–336.

GEIGER, T. and BISCHOFF,, A. (1989a): (Os, Ru, Ir)S_x and other refractory siderophile element-rich particles in the metamorphosed carbonaceous chondrites, Karoonda, Mulga (west), and PCA82500. Lunar and Planetary Science XX. Houston, Lunar Planet. Inst., 335–336.

GEIGER, T. and BISCHOFF, A. (1989b): Mineralogy of metamorphosed carbonaceous chondrites. Meteoritics, **24**, 269–270.

GEIGER, T. and BISCHOFF, A. (1990): Exsolution of spinel and ilmenite in magnetites from type 4-5 carbonaceous chondrites-Indications for metamorphic processes. Lunar and Planetary Science XXI. Houston, Lunar Planet. Inst., 409–410.

GEIGER, T. and BISCHOFF, A. (1991a): Maralinga–A new metamorphosed carbonaceous chondrite. Lunar and Planetary Science XXII. Houston, Lunar Planet. Inst., 433–434.

GEIGER, T. and BISCHOFF, A. (1991b): The CK chondrites-Conditions of parent body metamorphism. Meteoritics, **26**, 337.

GEIGER, T., BISCHOFF, A., SPETTEL, B. and BEVAN, A. W. R. (1992): Cook 003: A new CK chondrite from the Nullarbor Region, South Australia. Lunar and Planetary Science XXIII. Houston, Lunar Planet. Inst., 401–402.

HEYSE, J. V. (1978): The metamorphic history of LL-group ordinary chondrites. Earth Planet. Sci. Lett., **40**, 365–381.

HOUSLEY, R. M. and CIRLIN, E. H. (1983): On the alteration of Allende chondrules and the formation of matrix. Chondrules and Their Origins, ed. by E. A. KING. Houston, Lunar Planet. Inst., 145–161.

JOHNSON, C. A. and PRINZ, M. (1991): Chromite and olivine in type II chondrules in carbonaceous and ordinary chondrites: Implications for thermal histories and group differences. Geochim. Cosmochim. Acta, **55**, 893–904.

KALLEMEYN, G. W., RUBIN, A. E. and WASSON, J. T. (1991): The compositional classification of chondrites: V. The Karoonda (CK) group of carbonaceous chondrites. Geochim. Cosmochim. Acta, **55**, 881–892.

KELLER, L. P. (1992): Petrography and mineral chemistry of calcium- and aluminum-rich inclusions in the Maralinga CK4 chondrite. Lunar and Planetary Science XXIII. Houston, Lunar Planet. Inst., 671–672.

KELLER, L. P., CLARK, J, C., LEWIS, C. F. and MOORE, C. B. (1992): Maralinga, a metamorphosed carbonaceous chondrite found in Australia. Meteoritics, **27**, 87–91.

MACPHERSON, G. J. and DELANEY, J. S. (1985): A fassaite-two olivine-pleonaste-bearing refractory inclusion from Karoonda. Lunar and Planetary Science XVI. Houston, Lunar Planet. Inst., 515–516.

MACPHERSON, G. J., WARK, D. A. and ARMSTRONG, J. T. (1988): Primitive material surviving in chondrites: Refractory inclusions. Chondrites and the Early Solar System, ed. by J. F. KERRIDGE and M. S. MATTHEWS. Tucson, Univ. Arizona Press, 746–807.

MCCOY, T. J., SCOTT, E. D. R., JONES, R. H., KEIL, K. and TAYLOR, G. J. (1991): Composition of chondrule silicates in LL3-5 chondrites and implications for their nebular history and parent body metamorphism. Geochim. Cosmochim. Acta, **55**, 601–619.

NOGUCHI, T. (1987): Texture and chemical composition of pyroxenes in ordinary chondrites. Papers Presented to the 16th Symposium on Antarctic Meteorites, June 8–10, 1987. Tokyo, Natl Inst. Polar Res., 48–50.

NOGUCHI, T. (1989): Texture and chemical composition of pyroxenes in chondrules in carbonaceous and unequilibrated ordinary chondrites. Proc. NIPR Symp. Antarct. Meteorites, **2**, 169–199.

OKADA, A. (1975): Petrographical studies of the Yamato meteorites Part 1. Mineralogy of the Yamato meteorites. Mem. Natl Inst. Polar Res., Spec. Issue, **5**, 14–66.

RUBIN, A. E. (1992): A shock-metamorphic model for silicate darkening and compositionally variable plagioclase in CK and ordinary chondrites. Geochim. Cosmochim. Acta, **56**, 1705–1714.

SCOTT, E. R. D. and TAYLOR, G. J. (1985): Petrology of types 4-6 carbonaceous chondrites. Proc. Lunar Planet. Sci. Conf., 15th, Pt. 2, C699–C709 (J. Geophys. Res., **90**, Suppl.).

SCOTT, E. R. D., KEIL, K. and STÖFFLER, D. (1991): Shock metamorphism of carbonaceous chondrites. Lunar and Planetary Science XXII. Houston, Lunar Planet. Inst., 1207.

TAKEDA, H., HUSTON, T. J. and LIPSCHUTZ, M. E. (1984): On the chondrite-achondrite transition: mineralogy and petrology of Yamato-74160 (LL7). Earth Planet. Sci. Lett., **71**, 329–339.

TSUCHIYAMA, A., FUJITA, T. and KITAMURA, M. (1988): Fe-Mg heterogeneity in the low-Ca pyroxenes during metamorphism of the ordinary chondrites. Proc. NIPR Symp. Antarct. Meteorites, **1**, 173–184.

VAUGHAM, D. J. and CRAIG, J. R. (1978): Mineral chemistry of mineral sulfides. London, Cambridge Univ. Press, 493 p.

WEISBURG, M. K., PRINZ, M., KOJIMA, H., YANAI, K., CLAYTON, R. N. and MAYEDA, T. K. (1991): The Carlisle Lakes-type chondrites: A new grouplet with high $\Delta^{17}O$ and evidence for nebular oxidation. Geochim. Cosmochim. Acta, **55**, 2657–2669.

WOOD, J. A. and HASHIMOTO, A. (1988): The condensation sequence under non-classic conditions ($P < 10^{-3}$ atm, non-cosmic compositions). Lunar and Planetary Science XIX. Houston, Lunar Planet. Inst., 1292–1293.

YABUKI, H., EL GORESY, A. and RAMDOHR, P. (1983): A petrologic microprobe survey of coexisting olivines, pyroxenes, and spinels in L- and LL- chondrites. Meteoritics, **18**, 426–428.

(Received October 14, 1992; Revised manuscript received January 21, 1993)